THE CRYSTAL STRUCTURE OF SODIUM TRIPHOSPHATE HEXAHYDRATE

Thesis by

David Ray Dyroff

In Partial Fulfillment of the Requirements

For the Degree of

Doctor of Philosophy

California Institute of Technology

Pasadena, California

1965

(Submitted May 10, 1965)

ACKNOWLEDGMENTS

I thank Dr. Edward W. Hughes for his help and guidance as my faculty advisor.

I express my appreciation to the National Science Foundation for financial assistance.

I am grateful to the following people who contributed to computer programs which were used in this work: Dr. R. E. Marsh, Mr. D. J. Duchamp, Dr. N. C. Webb, Mr. A. P. Kendig, Dr. C. M. Gramaccioli, Mr. T. A. Beineke, and Mr. J. K. Lo.

I thank Dr. C. Y. Shen of the Monsanto Company for supplying raw materials and suggesting methods for preparing the crystals.

For helpful discussions, I am also grateful to Dr. R. E. Marsh, Mr. D. J. Duchamp, Dr. S. Samson, Mr. T. A. Beineke, Mr. C. T. Lin, and Dr. B. D. Sharma.

Finally, I wish to thank my parents, Erwin and M. Pauline Dyroff, and my wife, Corinne, for encouragement and support both during and previous to the work on this thesis.

ABSTRACT

The crystal structure of sodium triphosphate hexahydrate was determined by X-ray crystallographic methods. The crystals are triclinic with two $Na_5P_3O_{10} \cdot 6H_2O$ per unit cell in space group $P\bar{1}$. The structure of the anion was determined much more accurately than in other triphosphate structures done previously, and the unexpectedly large difference in length of the two types of P-O chain bond was confirmed. The P-O-P angle was 123.5°, which is closer than the previously reported values to what is observed in other kinds of phosphates. Sodium coordination is fivefold and sixfold. An unusual feature of the hydrogen bonding is that two of the phosphate oxygen atoms accept four hydrogen bonds each. Several macroscopic properties of the crystals are explained in terms of the crystal structure.

TABLE OF CONTENTS

THE CRYSTAL STRUCTURE OF SODIUM TRIPHOSPHATE HEXAHYDRATE

INTRODUCTION

Sodium triphosphate, $Na_5P_3O_{10}$, occurs in two anhydrous forms and as the hexahydrate. All three forms find extensive application in the detergent industry, and for this reason their physical properties and preparations have been extensively studied[1]. The structures of the anhydrous forms had already been determined[2, 3]. Thus, it was expected that the determination of the hydrate structure might provide some interesting comparisons among the three structures as well as some explanations of their macroscopic behavior. Of particular interest were the great difference in hydration rates of the two anhydrous forms and the difficulty in dehydrating the hydrate without destroying the triphosphate anion[4]. Because the anhydrous structures were based upon very little data, the present work was expected to yield improved values for the bond lengths and angles in the anion. Finally, it was expected that hydrogen bonding was present and might be of interest.

---

1 J. R. Van Waser, Phosphorus and Its Compounds, Interscience Publishers, New York (1958), Vol. 1, pp. 642-654.

2 D. R. Davies and D. E. C. Corbridge, Acta Cryst. 11, 315 (1958).

3 D. E. C. Corbridge, Acta Cryst. 13, 263 (1960).

4 C. Y. Shen, J. S. Metcalf, and E. V. O'Grady, Ind. Eng. Chem. 51, 717 (1959).

EXPERIMENTAL

Preparation of Single Crystals

All preparative methods which were tried produced only triclinic twins. Large twins consisting of just two individuals sharing a face (001) could be selected from crystals prepared by the following method suggested by Dr. C. Y. Shen of the Monsanto Chemical Company who also supplied the starting material.

Twenty grams of sodium trimetaphosphate, $Na_3P_3O_9$, were added to eighty grams of water at room temperature. Solids which could not be dissolved were filtered out, and a solution of 5.22 grams of sodium hydroxide in an equal weight of water was added with stirring. Crystals of $Na_5P_3O_{10} \cdot 6H_2O$ appeared overnight and grew slowly as more triphosphate was generated by hydrolytic cleavage of the trimetaphosphate. The crystals were lath-like with the longest dimension parallel to the b axis and the shortest parallel to the c axis.

Single crystals were isolated by washing away one of a pair of twins by rubbing with filter paper moistened with water. The process was monitored with a polarizing microscope. Three such crystals were mounted, each with a different crystallographic axis parallel to the rotation axis. These were then shaped into circular cylinders by further washing.

Unit Cell and Space Group

The a and c axis crystals used for measurements of the triclinic unit cell were approximately circular cylinders 0.1 mm. in

diameter. The b axis crystal was acicular with the diameter varying between 0.033 mm. and 0.067 mm. Zero layer precision Weissenberg photographs were obtained at room temperature for all three axes using the Straumanis arrangement with a camera ten centimeters in diameter. An optical comparator was used to measure the relative spot positions needed to calculate the effective camera radius and the following d spacings: (100), (010), (001), $(1\bar{1}0)$, $(10\bar{1})$, and $(01\bar{1})$. Wavelengths used were copper $K\alpha_1$ = 1.54051 Å and $K\alpha_2$ = 1.54433 Å. Values of each spacing based upon several high order reflections were plotted against the Nelson-Reilly function[5] and extrapolated to $\theta = 90^\circ$.

Various unit cell parameters, calculated with formulas given by Buerger[6], are given in Table I, along with some values obtained earlier by Bonneman and Bassière[7] using twinned crystals.

The calculated density for two $Na_5P_3O_{10} \cdot 6H_2O$ in the unit cell is 2.07 g. cm.$^{-3}$. The experimental value of Bonneman and Bassière[7] was 2.12 g. cm.$^{-3}$.

Intensity statistics[8] applied to the $h0\ell$ data indicated a center of symmetry (Figure 1); so the space group $P\bar{1}$ was chosen tentatively.

---

5 International Tables for X-Ray Crystallography, The Kynoch Press, Birmingham, England (1959), Vol. II, pp. 218, 228-229.

6 M. J. Buerger, X-Ray Crystallography, John Wiley and Sons, New York (1942), pp. 463-464.

7 P. Bonneman and M. Bassière, Comptes Rendus 206, 1379 (1938).

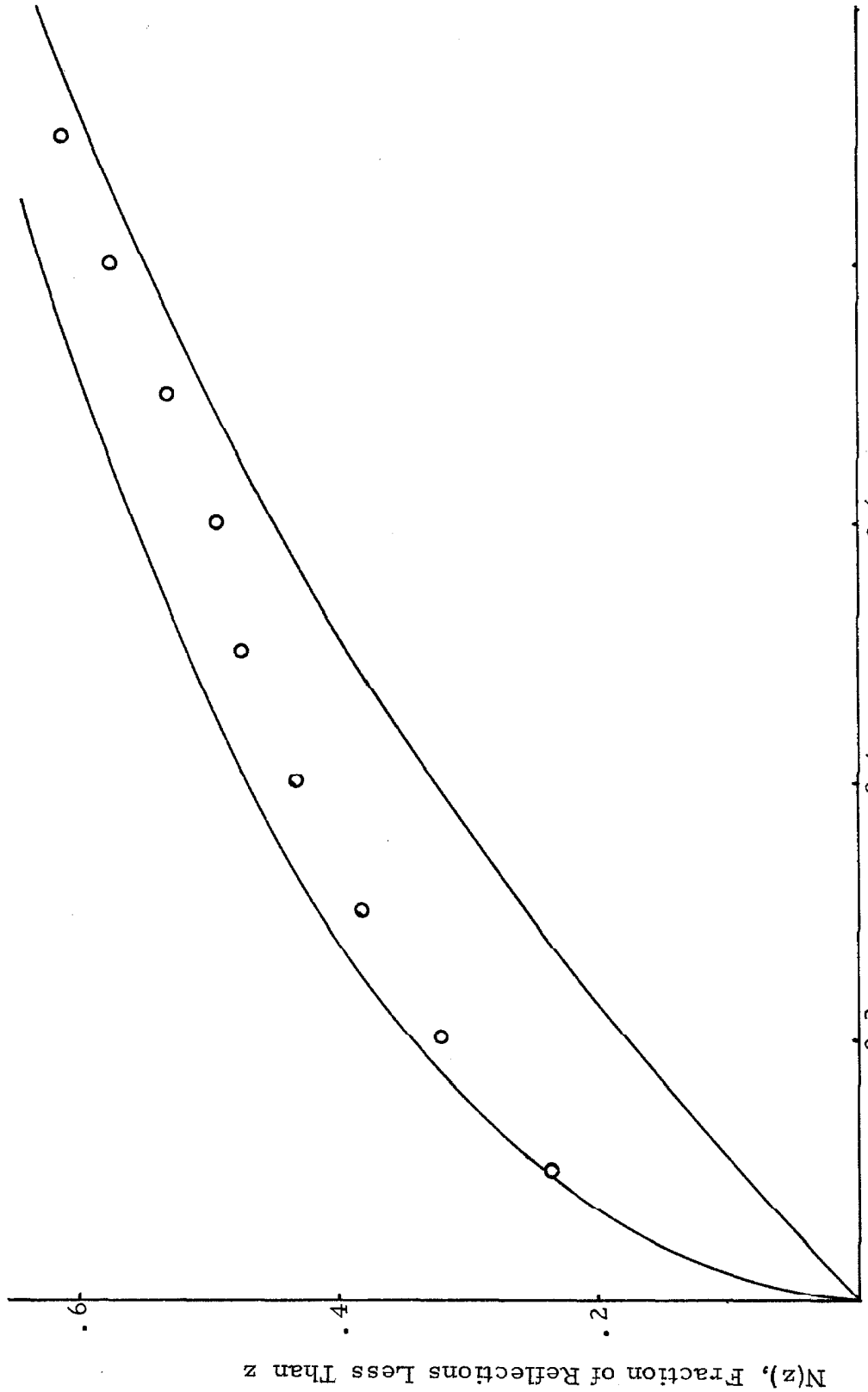

Figure 1. Howells-Phillips-Rogers Statistical Test.

Table I. Unit Cell Parameters

Parameter	Present Value	Earlier Value[7]
a	7.572 ± .001 Å	
b	9.801 ± .001 Å	
c	10.308 ± .001 Å	10.23 ± .05 Å
α	90° 55' ± 1'	
β	94° 29' ± 1'	
γ	92° 14' ± 1'	
d (100)	7.543 ± .001 Å	7.53 ± .04 Å
d (010)	9.792 ± .001 Å	9.83 ± .05 Å
γ*	87° 41' ± 1'	87° 30'
V	762 Å^3	757 ± 12 Å^3

Intensity Data

Layers zero through fourteen were photographed about the b and c axes by the equi-inclination Weissenberg method using molybdenum radiation filtered through zirconium. One pack of four films interleaved with .001-inch nickel foils was used for each set of photographs.

The intensities were estimated visually using only the spots on the upper half of each film (that is, those which were extended by the Weissenberg motion). Graduated intensity scales were prepared with the same crystals used for the photographs. No correction for spot shape or size was applied, but the spots were viewed without magni-

[8] E. Howells, D. Phillips, and D. Rogers, Acta Cryst. 3, 210 (1950).

fication from a distance great enough to allow the eye to integrate over each spot. Doubtful observations were either assigned low weight or eliminated, depending upon the quality of other observations of the same intensity. The weak ends of the intensity strips were used only for the first film of a pack, and the strong ends were used only for the fourth film.

The b axis crystal was a cylinder 0.27 mm. in diameter, and the c axis crystal was a cylinder 0.37 mm. in diameter. Since the calculated linear absorption coefficient was only 0.642 $mm.^{-1}$, absorption errors could be neglected. Exposures for the b axis varied between 71 hours for the zero layer and about 120 hours for the fifth and higher layers. Exposures for the c axis varied between 41.7 hours for the zero layer and about 95 hours for the eighth and higher layers. No radiation damage to the crystals was noticed.

Iron radiation was used with the crystals used for unit cell measurements to collect the low angle data which was not on the molybdenum films. This less accurate data, given in Table II, was used only for the Patterson function.

Table II. Structure Factors Obtained with Iron Radiation

(The scale is the same as that for the data in Appendix A.)

Index			F	Index			F
0	2	-3	27.	-1	1	1	35.
0	1	-2	2.1	-1	2	1	34.
0	2	-2	15.	0	0	1	34.
1	0	-2	40.	0	1	1	31.

Index			F	Index			F
1	1	-2	40.	0	2	1	13.
1	2	-2	37.	1	-2	1	17.
0	1	-1	29.	1	-1	1	34.
0	2	-1	5.5	1	0	1	32.
1	0	-1	46.	1	1	1	22.
1	1	-1	44.	1	2	1	3.6
1	2	-1	28.	-1	1	2	31.
2	1	-1	3.1	-1	2	2	36.
0	1	0	small	0	0	2	27.
0	2	0	58.	0	1	2	14.
1	-2	0	24.	0	2	2	7.7
1	-1	0	19.	1	-2	2	2.5
1	0	0	32.	1	-1	2	21.
1	1	0	13.	1	1	2	5.3
1	2	0	42.	1	2	2	27.
-2	1	1	28.	0	0	3	10.

Twinning and Distortion

An optical goniometer was used to study the twinning on the (001) face. The interfacial angles for each individual gave the orientation of the axes and indicated that the c* axes coincided, while the a axes pointed in opposite directions. That is, the twins are related by a rotation of 180° about the c* axis. As a check, the following angles were measured:

Axes forming the angle	calculated	observed	discrepancy
c*, c* (twin)	0° 0'	0° 27'	0° 27'
a*, -a* (twin)	9° 3'	8° 56'	0° 7'
b*, -b* (twin)	2° 11'	2° 10'	0° 1'

The agreement seems acceptable.

Another type of twinning was reported by Bonneman and Bassière[7] in which the c axes and (100) faces of the twins coincide. In the present work, multiple twinning on the (100) face was also observed but not studied in detail. It was, however, noticed that this type of twinning could sometimes be removed or produced by pressure.

A third type of crystal was noticed, but not studied, in which, moving along the b direction, the a and c axes seemed to twist continuously about the b axis.

DATA REDUCTION

Data Tape Preparation

All computer calculations were done by the CRYRM Crystallographic Computing System[9] recently developed at the California Institute of Technology. First, factors were calculated for scaling within a pack of films. These film factors were applied to the intensities along with the Lorentz and polarization factors. Then, all data was scaled together and averaged intensities were calculated. Finally, a data tape was prepared containing, for each independent reflection, the structure factor, a least squares weight, form factors, and other information. This tape was used in all subsequent calculations requiring structure factor information.

Modifications were made in the programs to allow more data to be processed. Also, in order not to exceed the capacity of the final data tape, reflections with $(\sin^2\theta)\lambda^{-2}$ greater than 1.267 were omitted if they had been observed only as less than some value.

Film Factors

The computer calculated a separate set of three film factors for each pack of four films. The film factor k is expected to increase with increasing equi-inclination angle μ, from a value of k_o for the zero layer, according to the function

$$k = k_o^{(\sec.\,\mu)} .$$

---

9 D. J. Duchamp, Abstracts A. C. A. Bozeman Meeting, 1964, B 14, p. 29.

Thus a plot of log k versus secant μ should fit a straight line of slope log k_o. This was so, but k_o was different for each of the three factors of a pack and, to a smaller extent, for the same factor on the two axes. Also, there was a nonrandom deviation from the theoretical curve for small μ, as can be seen in Figure 2. The three different values of k_o for each axis are understandable because of differences in background radiation and environment of the four films caused largely by the nickel foils. However, the other deviations have not been explained.

Since film factors depend partly upon the observer, and since the state of the observer must vary, the individual film factors seemed more reliable than those read from theoretical curves. Yet, statistics favored the theoretical values. It was decided to use a weighted average of the two values which favored the individual values except when they were based upon a rather small number of observations, in which case the theoretical values predominated.

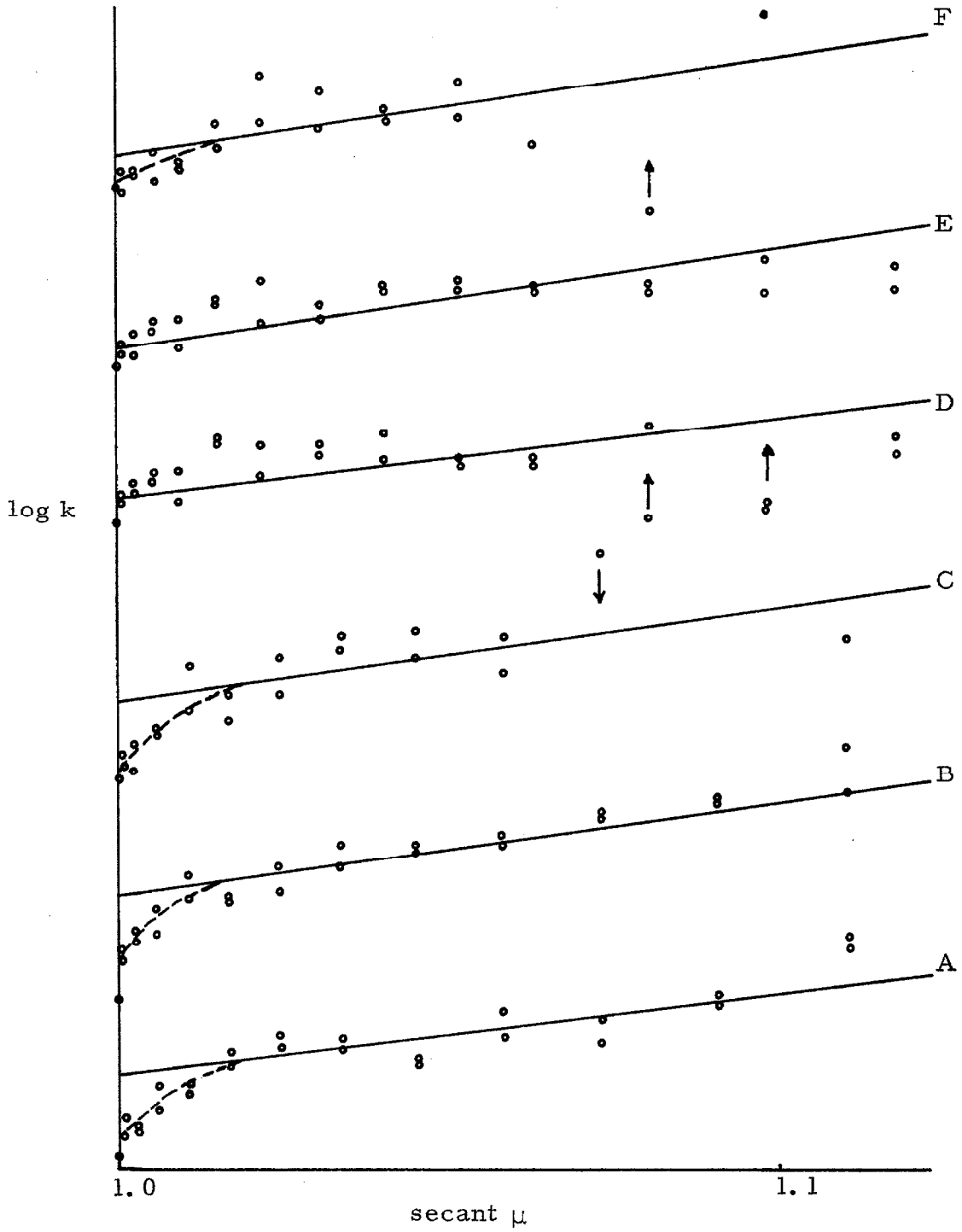

Figure 2. Film Factor k as a Function of Equi-inclination Angle μ. In each case, the solid line is the theoretical curve best fitted to the nondeviant points. A. Axis b, film 1 to film 2, $k_0 = 3.13$. B. Axis b, film 2 to film 3, $k_0 = 3.70$. C. Axis b, film 3 to film 4, $k_0 = 3.66$. D. Axis c, film 1 to film 2, $k_0 = 3.01$. E. Axis c, film 2 to film 3, $k_0 = 3.71$. F. Axis c, film 3 to film 4, $k_0 = 3.94$.

TRIAL STRUCTURE

The sharpened, three-dimensional Patterson function, with the peak at the origin removed, was calculated using scale and temperature factors obtained by Wilson's method[10]. In examining the structures of anhydrous sodium triphosphate[2,3], it was discovered that the distance between adjacent phosphorus atoms in the anion, 2.87 Å, was quite different from any other distance expected in the hexahydrate which involved an atom heavier than oxygen. Circles were drawn on the contoured Patterson sections representing points 2.87 Å away from the origin; and as expected for the known anion configuration, exactly two peaks fell on the circles. This agreed with the assumed symmetry, $P\bar{1}$, and gave the rotational orientation of the anions.

Next, the positions of the six largest unassigned peaks were determined, and all possible vector sums and differences of these six vectors were compared with the three known vectors within an anion, $\overrightarrow{P_iP_j}$. Any two vectors, $\overrightarrow{P_iP_j'}$, between atoms in different anions must combine to give one of the vectors $\overrightarrow{P_iP_j}$. Four of the six unknown vectors did so and were assumed to be of the type $\overrightarrow{P_iP_j'}$.

Since the three phosphorus atoms in an anion define a plane, all the peaks P_iP_j' had to lie in a plane. A Patterson section containing the four assumed P_iP_j' peaks was prepared, which included in addition only some of the larger peaks. Three peaks resembling the arrangement of phosphorus atoms in an anion were found and were

---

10 A. J. C. Wilson, Nature 150, 152 (1942).

assumed to be a set of peaks P_iP_1', P_iP_2', and P_iP_3'. The choice among the three possible assignments of these peaks was made by trial and error, leading to the location of the phosphorus atoms and the assignment of all PP peaks. It was possible then to adjust the coordinates of the phosphorus atoms to give excellent agreement with all PP peaks.

A model of the structure was begun, and atoms were added to it as they were located. The oxygen atoms in the anion were easily located with the help of the model since the anion structure was approximately known. Each oxygen position was adjusted to give the best agreement with all the PO peaks. Two sodiums and one water molecule were located by inspection of the model and verified with the Patterson.

The rest of the sodiums and another water molecule were located as follows. An unassigned, well-resolved Patterson peak was chosen, and its coordinates were added to those of each of the known atoms except one. Then the coordinates of the excepted atom were subtracted. Unless the chosen peak represented a vector between two unknown atoms, unlikely at that stage, the procedure would eventually result in the coordinates of another unassigned peak. Then the coordinates of the new atom were given by the sum of the coordinates of the first peak and those of the known atom which led to the second peak.

Four water molecules could not be reliably located with the Patterson; so a structure factor calculation was done with the rest of the atoms. These signs were used for a three-dimensional Fourier synthesis in which reflections with $(\sin^2\theta)\lambda^{-2}$ greater than 0.29 or

with |F calc.| less than ten were omitted. All of the atoms known previously appeared as well as four and only four new ones. This completed the trial structure.

REFINEMENT

Each stage of the refinement was continued until the parameter shifts and the decrease in the reliability factors per cycle were small.

Heavy atom positions were refined first, starting from the coordinates listed under cycle zero in Table III which had been obtained from Patterson and Fourier maps. The initial temperature factor, $B = 0.778$ Å^2, had been estimated by Wilson's method[10]. Next, individual isotropic temperature factors were refined starting from the overall value.

A difference Fourier map was prepared, and the distances from the water oxygens to surrounding oxygens were calculated. Eleven short distances were found which were all in positions such that they could reasonably be assumed to be hydrogen bonds. Ten hydrogens could be located in the difference Fourier including the one forming no hydrogen bond. The hydrogens on W(5) were obscured by its large anisotropic thermal vibration. The initial hydrogen coordinates in Table III were chosen to give the best agreement with the difference Fourier, with assumed hydrogen bond positions, and with the expected structure of a water molecule. Arbitrary initial temperature factors of $B = 2.0$ Å^2 were used for all hydrogens except for those on W(5) which were assumed twice as large.

Hydrogen atoms were included without refinement in subsequent structure factor calculations until anisotropic temperature factors for the heavy atoms had been refined using all the data. Refinement of hydrogen positions was begun with all other parameters held fixed using only data with $(\sin^2\theta)\lambda^{-2}$ less than 0.2 Å^{-2}. Then hydro-

gen isotropic temperature factors were refined along with the hydrogen positions. Finally, in the remaining cycles, all parameters were refined using all the data.

A final difference Fourier synthesis indicated no serious errors in the structure since the largest peak was -0.69 electrons at a position where there was no atom. The final least squares shifts, expressed as fractions of the corresponding standard deviations, were as follows:

Parameters	Maximum $\Delta_i \sigma_i^{-1}$	Average $\Delta_i \sigma_i^{-1}$
heavy atom coordinates	.260	.067
heavy atom thermal parameters	.525	.133
hydrogen positions	.502	.125
hydrogen temperature factors	.256	.124
scale factor	.53	.53

The definitions and final values of several reliability factors are given in Table III.

The final parameters and their standard deviations are given in Tables III and IV. Further details of the refinement are given below and in Table III. In this discussion, an observed reflection is one which was estimated as equal to some value, and an unobserved reflection is one which was estimated only as less than some value.

Under the CRYRM crystallographic computing system[9], the function minimized during least squares refinement is

$$\Sigma w(k^2|F_{obs}|^2 - |F_{calc}|^2)^2$$

where k is the scale factor for F_{obs} and w is the weight. The weights on the data tape[9] used during most of the refinement, are meant to obey as nearly as possible the following relationship to the standard deviations of the observations.

$$w^{-0.5} = \sigma(|F_{obs}|^2)$$

During the first four cycles, the Hughes F_{obs}^{-1} weights[9] were used, for which, except for weak reflections,

$$w^{-0.5} = F_{obs} .$$

In the refinement and in the calculations of reliability factors and standard deviations, the unobserved reflections were included only when the calculated structure factors exceeded the observed upper limits. Zero weight reflections affected none of these calculations.

The standard deviations given in Tables III and IV were calculated with the equation

$$\sigma_i^2 = (A^{-1})_{ii}(m-s)^{-1}\Sigma w(k^2|F_{obs}|^2-|F_{calc}|^2)^2$$

where m is the number of observations, s is the number of parameters refined, and $(A^{-1})_{ii}$ is the diagonal element of the inverse matrix corresponding to parameter i . The final goodness of fit (Table III) should be unity if refinement is complete and the weights are correct. In this case, it was close to unity, which implies that the standard deviations are not appreciably in error as a result of incorrect weights. In the last two least-squares cycles, each set of three

coordinates occupied a separate block of the matrix; and the set of thermal parameters for each atom occupied a separate block, except that the thermal parameters of the phosphorus and sodium atoms were in a single block along with the scale factor. The neglect of some off-diagonal matrix elements will tend to make the estimated standard deviations too small, but in this case any such errors should certainly be less than ten per cent.

The atomic scattering factors used for this refinement (H, O, P, Na^{+}, and $O^{-0.5}$) were contained in the CRYRM system[9] and were taken from the International Tables[11]. The $O^{-0.5}$ scattering factor, used for the phosphate oxygens, is an interpolation between those for O and O^{-1}.

The data reduction program gave zero weight to 367 reflections. Another 500, mostly weak or very strong reflections, were given zero weight at various stages of the refinement. In each case, there was some reason for unreliability in addition to a lack of agreement between the observed and calculated values. For 271 reflections, the reason was extinction. Of these reflections, those for which $Q > 6000$ are included in the plot of $\log(F_{calc}F_{obs}^{-1})$ versus Q in Figure 3, where $Q = |F_{calc}|^2(1+\cos^2 2\theta)$. For small Q, the points fit a straight line through the origin as they should for secondary extinction[12]. The deviation for large Q is in the direction

---

11 International Tables for X-Ray Crystallography, The Kynoch Press, Birmingham, England (1962), Vol. III, pp. 202-203.

12 International Tables for X-Ray Crystallography, The Kynoch Press, Birmingham, England (1959), Vol. II, pp. 313-314.

which would result from primary extinction. Considerable scatter is expected due to variations in path length which were ignored for this plot.

Zero weight was also assigned if:

1. The original observation had been marked as questionable.
2. Something else had been mistaken for a diffraction spot.
3. A spot which should have been equivalent to the one in question was missing or much weaker.
4. The spot shape or position was abnormal.
5. Anomalous dispersion effects were unusually large.
6. The spot was obscured by background or white radiation streaks.
7. An indexing or recording error had been made.
8. Re-estimation gave a considerably different result.

There were no modifications of the data during refinement other than assignments of zero weight. Although zero weight reflections don't affect the refinement, they are included in all lists of F_{calc} and F_{obs}. Forty low angle data obtained with iron radiation were used only for the Patterson function and are not included in the lists, but a structure factor calculation after cycle three gave an R factor for these reflections of 18.8 per cent, indicating satisfactory agreement in view of the inaccurate scaling and large extinction errors for these data. The values of F_{obs} and the final values of F_{calc} for all reflections except these forty are given in Appendix A.

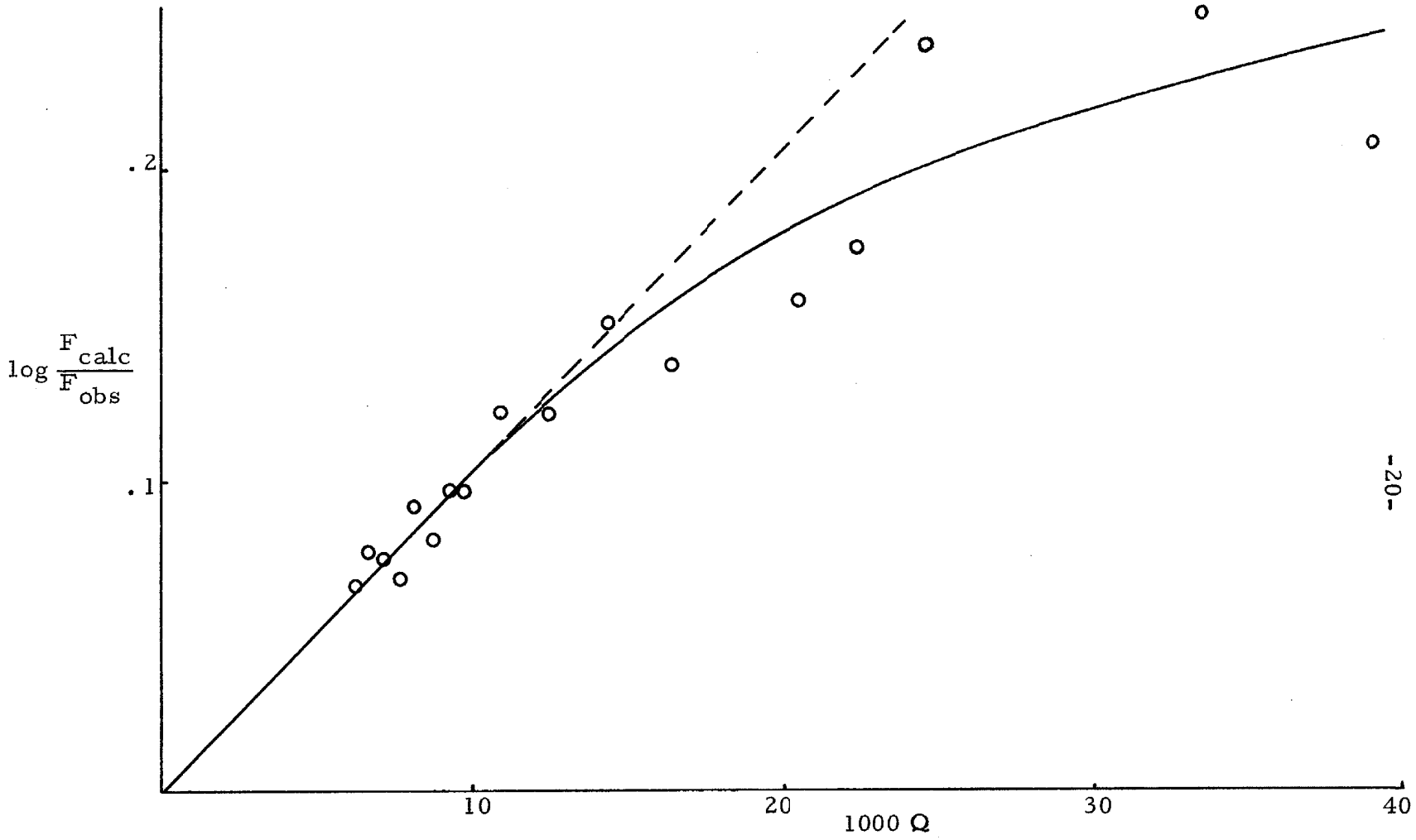

Figure 3. Extinction. Data with $Q > 6000$ were divided into intervals of 500 in Q for $Q < 10,000$ and intervals of 2000 elsewhere. Each interval is represented by one point with the average ordinate and average Q for all reflections within the interval. Points at high Q are missing or unreliable due to scarcity of data. $Q = |F_{calc}|^2(1+\cos^2 2\theta)$.

Table III. Summary of the Refinement

Cycle Number	0	4	9	11
$(\sin^2\theta)\lambda^{-2}$ max. in $Å^{-2}$	0.3	0.3	0.5	0.5
Refined Parameters:				
coordinates	none	heavy atoms	heavy atoms	heavy atoms
heavy atom thermal	none	none	iso.	iso.
scale factor	no	yes	yes	yes
Fixed Parameters:				
coordinates	heavy atoms	none	none	hydrogens
heavy atom thermal	overall iso.	overall iso.	none	none
hydrogen thermal	none	none	none	iso
R *	22.1	14.2	7.83	7.76
R' *	24.6	8.58	3.64	3.50
Goodness of Fit *	23.8	14.3	2.12	2.03
Number of Data:				
total included	2111	2111	4469	4469
observed, nonzero weight	1869	1869	3723	3723

* $R = \Sigma\left|\,|kF_{obs}| - |F_{calc}|\,\right| \div \Sigma kF_{obs}$ $\qquad R' = \Sigma w(k^2|F_{obs}|^2 - |F_{calc}|^2)^2 \div \Sigma w|F_{obs}|^4$

$(\text{goodness of fit})^2 = \Sigma w(k^2|F_{obs}|^2 - |F_{calc}|^2)^2 \div k^4(m-s)$

where k is the scale factor, w is the weight, m is the number of observations, and s is the number of parameters refined.

Table III. (cont'd.)

Number of Data (cont'd.)				
unobserved	193	193	680	680
unobserved, calc. too big	75	41	27	24
Type of Matrix		full	full	full
Cycle Number	23	30	38	38 (Cu sphere)
$(\sin^2\theta)\lambda^{-2}$ max. in Å^{-2}	1.9	1.9	1.9	0.42
Refined Parameters:				
coordinates	heavy atoms	all	all	
heavy atom thermal	aniso.	aniso.	aniso.	
hydrogen thermal	none	iso.	iso.	
scale factor	yes	yes	yes	
Fixed Parameters:				
coordinates	hydrogens	none	none	
heavy atom thermal	none	none	none	
hydrogen thermal	iso.	none	none	
R*	6.23	5.66	5.61	4.48
R'*	1.55	1.28	1.24	1.18
Goodness of Fit*	0.987	0.907	0.884	1.19

* $R = \Sigma\left|\,|kF_{obs}|-|F_{calc}|\,\right| \div \Sigma kF_{obs}$ $\qquad R' = \Sigma w(k^2|F_{obs}|^2-|F_{calc}|^2)^2 \div \Sigma w|F_{obs}|^4$

(goodness of fit)$^2 = \Sigma w(k^2|F_{obs}|^2-|F_{calc}|^2)^2 \div k^4(m-s)$, where k is the scale factor, w is the weight, m is the number of observations, and s is the number of parameters refined.

Table III. (cont'd.)

Number of Data:				
total included	18,857	18,857	18,857	3440
observed, nonzero weight	9,079	8,893	8,892	2677
unobserved	9,098	9,098	9,098	439
unobserved, calc. too big	132	120	113	1
Type of Matrix	block	block	block	block

Cycle Number	0	4	9	11	23	30	38	(1000 σ)*
P(1)								
x	.740	.741	.741	.741	.741	.7409	.74090	.04
y	.256	.253	.253	.253	.253	.2534	.25335	.03
z	.609	.609	.609	.609	.609	.6090	.60901	.03
P(2)								
x	.949	.951	.952	.952	.952	.9521	.95210	.04
y	.260	.267	.266	.266	.266	.2658	.26580	.03
z	.854	.852	.852	.852	.852	.8523	.85236	.03
P(3)								
x	.280	.281	.281	.281	.281	.2810	.28099	.04
y	.238	.237	.237	.237	.237	.2370	.23702	.03
z	.005	.004	.004	.004	.004	.0041	.00411	.03
Na(1)								
x	.916	.912	.911	.912	.911	.9115	.91152	.08
y	.070	.065	.066	.066	.066	.0656	.06554	.06
z	.122	.119	.119	.119	.119	.1193	.11938	.06

* σ = standard deviation

Table III. (cont'd.)

Cycle Number	0	4	9	11	23	30	38	(1000 σ)*
Na(2)								
x	.955	.951	.951	.950	.950	.9503	.95030	.08
y	.406	.411	.412	.412	.412	.4115	.41154	.06
z	.134	.133	.134	.134	.134	.1337	.13382	.06
Na(3)								
x	.577	.586	.585	.585	.585	.5848	.58470	.08
y	.076	.062	.063	.062	.063	.0626	.06259	.07
z	.865	.861	.862	.862	.861	.8615	.86141	.07
Na(4)								
x	.233	.230	.229	.229	.230	.2296	.22954	.09
y	.243	.240	.242	.242	.241	.2415	.24145	.07
z	.340	.342	.342	.342	.342	.3424	.34241	.06
Na(5)								
x	.574	.578	.577	.578	.577	.5773	.57733	.08
y	.454	.451	.451	.450	.450	.4505	.45048	.06
z	.856	.855	.854	.854	.854	.8542	.85428	.06
O(1)								
x	.935	.932	.932	.932	.932	.9321	.9321	.1
y	.264	.268	.268	.269	.269	.2686	.2686	.1
z	.694	.698	.697	.697	.697	.6970	.6972	.1
O(2)								
x	.160	.164	.161	.161	.162	.1616	.1616	.1
y	.289	.288	.288	.288	.288	.2879	.2878	.1
z	.883	.873	.872	.872	.872	.8722	.8721	.1

* σ = standard deviation

Table III. (cont'd.)

Cycle Number	0	4	9	11	23	30	38	(1000 σ)*
O(3)								
x	.874	.871	.871	.871	.871	.8712	.8713	.1
y	.387	.385	.389	.389	.389	.3894	.3894	.1
z	.905	.906	.908	.908	.908	.9075	.9075	.1
O(4)								
x	.910	.897	.894	.894	.893	.8934	.8935	.1
y	.125	.131	.129	.129	.129	.1288	.1288	.1
z	.907	.897	.898	.898	.898	.8976	.8976	.1
O(5)								
x	.740	.742	.743	.743	.743	.7429	.7429	.1
y	.380	.378	.379	.379	.379	.3785	.3785	.1
z	.520	.524	.524	.524	.524	.5238	.5237	.1
O(6)								
x	.736	.746	.751	.751	.750	.7503	.7505	.1
y	.129	.123	.121	.121	.121	.1209	.1209	.1
z	.539	.533	.533	.533	.532	.5322	.5324	.1
O(7)								
x	.595	.600	.600	.600	.600	.6003	.6003	.1
y	.251	.252	.251	.251	.252	.2517	.2517	.1
z	.704	.705	.705	.705	.705	.7050	.7050	.1
O(8)								
x	.429	.434	.435	.435	.435	.4353	.4353	.1
y	.336	.341	.341	.341	.341	.3410	.3410	.1
z	.018	.015	.016	.016	.016	.0157	.0157	.1

* σ = standard deviation

Table III. (cont'd.)

Cycle Number	0	4	9	11	23	30	38	(1000 σ)
O(9)								
x	.325	.331	.332	.332	.332	.3322	.3323	.1
y	.098	.095	.094	.094	.094	.0942	.0943	.1
z	.969	.973	.972	.972	.971	.9712	.9713	.1
O(10)								
x	.158	.159	.161	.161	.161	.1610	.1609	.1
y	.227	.246	.245	.245	.245	.2449	.2449	.1
z	.107	.115	.114	.114	.114	.1140	.1139	.1
W(1)								
x	.713	.714	.714	.714	.715	.7147	.7148	.2
y	.252	.251	.251	.250	.250	.2504	.2505	.1
z	.166	.166	.167	.167	.167	.1666	.1665	.1
W(2)								
x	.992	.989	.988	.988	.988	.9881	.9880	.2
y	.065	.066	.066	.066	.066	.0659	.0659	.1
z	.346	.346	.346	.346	.346	.3459	.3457	.1
W(3)								
x	.010	.011	.011	.011	.010	.0106	.0106	.2
y	.420	.415	.416	.416	.416	.4155	.4155	.1
z	.364	.357	.356	.356	.356	.3562	.3562	.1
W(4)								
x	.455	.453	.455	.455	.454	.4540	.4540	.2
y	.425	.429	.428	.428	.429	.4286	.4286	.1
z	.345	.344	.345	.345	.345	.3448	.3449	.1

Table III. (cont'd.)

Cycle Number	0	4	9	11	23	30	38	(1000 σ)
W(5)								
x	.265	.265	.266	.266	.266	.2660	.2660	.2
y	.239	.243	.240	.240	.241	.2409	.2407	.3
z	.567	.569	.568	.568	.569	.5683	.5682	.2
W(6)								
x	.545	.540	.543	.543	.544	.5438	.5438	.2
y	.934	.931	.929	.929	.929	.9287	.9286	.1
z	.658	.658	.657	.657	.658	.6580	.6579	.1

Cycle Number	23 (initial positions)	30	38	(100 σ)
H(1)				
x	.705	.677	.667	.4
y	.280	.248	.232	.3
z	.262	.231	.222	.4
H(2)				
x	.620	.601	.600	.4
y	.277	.278	.277	.4
z	.102	.122	.122	.3
H(3)				
x	.060	.037	.036	.4
y	.991	.998	.998	.3
z	.379	.371	.372	.3

Table III (cont'd.)

Cycle Number	23 (initial positions)	30	38	(100 σ)
H(4)				
x	.900	.909	.909	.4
y	.081	.083	.083	.3
z	.414	.388	.388	.3
H(5)				
x	.096	.063	.065	.4
y	.488	.488	.489	.3
z	.388	.382	.383	.3
H(6)				
x	.914	.919	.920	.4
y	.395	.402	.399	.3
z	.424	.399	.398	.3
H(7)				
x	.551	.537	.539	.3
y	.387	.403	.404	.3
z	.401	.388	.389	.3
H(8)				
x	.394	.399	.399	.5
y	.488	.489	.491	.4
z	.403	.392	.390	.4
H(9)				
x	.376	.362	.363	.5
y	.244	.255	.251	.4
z	.628	.615	.618	.4

Table III (cont'd.)

Cycle Number	23 (initial positions)	30	38	(100 σ)
H(10)				
x	.162	.184	.185	.4
y	.250	.264	.261	.3
z	.623	.612	.612	.3
H(11)				
x	.455	.443	.445	.4
y	.893	.904	.905	.3
z	.583	.599	.602	.3
H(12)				
x	.613	.605	.603	.4
y	.009	.993	.991	.4
z	.628	.621	.620	.4

Table IV. Final Scale and Thermal Parameters

Scale Factor = 3.622, σ = .001

Anisotropic Temperature Factors:*

	$10^4 B_{ii}$	$10^4 \sigma$**		$10^4 B_{ij}$	$10^4 \sigma$**
P(1)					
B_{11}	29.9	.4	B_{12}	4.5	.4
B_{22}	21.8	.2	B_{13}	-1.0	.4
B_{33}	14.1	.2	B_{23}	-0.8	.3
P(2)					
B_{11}	25.8	.4	B_{12}	2.2	.4
B_{22}	15.9	.2	B_{13}	0.6	.4
B_{33}	13.3	.2	B_{23}	3.5	.3
P(3)					
B_{11}	20.6	.4	B_{12}	0.4	.4
B_{22}	16.9	.2	B_{13}	4.3	.4
B_{33}	15.7	.2	B_{23}	2.5	.3
Na(1)					
B_{11}	75.4	1.0	B_{12}	6.2	1.0
B_{22}	32.5	.5	B_{13}	5.3	1.1
B_{33}	29.0	.5	B_{23}	2.2	.8
Na(2)					
B_{11}	70.7	.9	B_{12}	-2.9	1.0
B_{22}	34.7	.5	B_{13}	14.1	1.1
B_{33}	29.4	.5	B_{23}	-5.0	.8
Na(3)					
B_{11}	53.9	.9	B_{12}	7.6	1.1
B_{22}	44.3	.5	B_{13}	25.1	1.0
B_{33}	37.1	.5	B_{23}	17.9	.8

* exp. $- (h^2B_{11}+k^2B_{22}+\ell^2B_{33}+hkB_{12}+h\ell B_{13}+k\ell B_{23})$

** σ = standard deviation

Table IV. (cont'd.)

	$10^4 B_{ii}$	$10^4 \sigma$		$10^4 B_{ij}$	$10^4 \sigma$
Na(4)					
B_{11}	71.6	1.0	B_{12}	10.4	1.2
B_{22}	49.4	.6	B_{13}	1.7	1.1
B_{33}	31.9	.5	B_{23}	1.1	.9
Na(5)					
B_{11}	62.3	.9	B_{12}	16.2	1.0
B_{22}	35.9	.5	B_{13}	22.7	1.0
B_{33}	32.4	.5	B_{23}	5.7	.8
O(1)					
B_{11}	33.0	1.1	B_{12}	4.3	1.4
B_{22}	40.0	.8	B_{13}	-3.6	1.3
B_{33}	15.0	.6	B_{23}	5.0	1.1
O(2)					
B_{11}	29.8	1.1	B_{12}	-3.9	1.4
B_{22}	39.7	.8	B_{13}	-4.8	1.3
B_{33}	19.8	.7	B_{23}	21.1	1.1
O(3)					
B_{11}	50.0	1.3	B_{12}	18.3	1.4
B_{22}	24.3	.7	B_{13}	3.1	1.5
B_{33}	27.0	.7	B_{23}	-11.4	1.1
O(4)					
B_{11}	47.4	1.2	B_{12}	-8.7	1.4
B_{22}	21.6	.6	B_{13}	4.1	1.5
B_{33}	31.1	.8	B_{23}	14.3	1.1
O(5)					
B_{11}	57.3	1.4	B_{12}	18.7	1.7
B_{22}	42.5	.9	B_{13}	2.0	1.7
B_{33}	31.4	.8	B_{23}	37.0	1.3

Table IV. (cont'd.)

	$10^4 B_{ii}$	$10^4 \sigma$		$10^4 B_{ij}$	$10^4 \sigma$
O(6)					
B_{11}	69.1	1.6	B_{12}	-10.1	1.8
B_{22}	37.6	.8	B_{13}	16.2	1.8
B_{33}	39.0	.9	B_{23}	-37.8	1.4
O(7)					
B_{11}	39.6	1.2	B_{12}	.0	1.5
B_{22}	40.6	.8	B_{13}	18.7	1.4
B_{33}	23.8	.7	B_{23}	.1	1.2
O(8)					
B_{11}	42.4	1.2	B_{12}	-26.4	1.5
B_{22}	30.9	.7	B_{13}	-4.9	1.5
B_{33}	30.3	.8	B_{23}	3.0	1.2
O(9)					
B_{11}	53.9	1.3	B_{12}	17.4	1.4
B_{22}	23.2	.7	B_{13}	15.4	1.6
B_{33}	34.3	.8	B_{23}	1.6	1.1
O(10)					
B_{11}	50.0	1.3	B_{12}	14.2	1.6
B_{22}	39.3	.8	B_{13}	20.0	1.5
B_{33}	19.3	.7	B_{23}	4.1	1.1
W(1)					
B_{11}	59.3	1.6	B_{12}	23.8	2.2
B_{22}	72.4	1.3	B_{13}	17.6	2.1
B_{33}	50.7	1.1	B_{23}	24.3	1.9
W(2)					
B_{11}	97.5	1.9	B_{12}	34.6	2.2
B_{22}	52.7	1.0	B_{13}	27.9	2.0
B_{33}	30.0	.9	B_{23}	12.0	1.5

Table IV. (cont'd.)

	$10^4 B_{ii}$	$10^4 \sigma$		$10^4 B_{ij}$	$10^4 \sigma$
W(3)					
B_{11}	93.0	1.8	B_{12}	-20.8	2.1
B_{22}	47.4	1.0	B_{13}	30.2	1.9
B_{33}	31.0	.9	B_{23}	-20.5	1.4
W(4)					
B_{11}	91.9	1.8	B_{12}	34.1	2.1
B_{22}	46.9	1.0	B_{13}	-19.0	2.0
B_{33}	31.7	.9	B_{23}	-6.6	1.4
W(5)					
B_{11}	72.8	2.2	B_{12}	36.4	4.5
B_{22}	259.8	4.0	B_{13}	-1.9	2.4
B_{33}	33.2	1.2	B_{23}	-14.6	3.3
W(6)					
B_{11}	99.6	1.9	B_{12}	-4.7	2.1
B_{22}	44.6	1.0	B_{13}	-5.3	2.1
B_{33}	36.2	.9	B_{23}	9.7	1.5

Isotropic Temperature Factors in $Å^2$

Atom	B	σ	Atom	B	σ
H_1	2.0	.6	H_7	.7	.5
H_2	2.2	.7	H_8	3.2	.8
H_3	1.2	.5	H_9	2.4	.7
H_4	1.4	.6	H_{10}	1.9	.6
H_5	1.0	.5	H_{11}	1.1	.5
H_6	.6	.5	H_{12}	2.2	.7

DISCUSSION OF RESULTS

Anion Structure

The general triphosphate ion configuration is shown in Figure 4. Distances and angles for the anion in $Na_5P_3O_{10} \cdot 6H_2O$ are given in Table V. No corrections were made for molecular angular oscillations. The estimation of the standard deviations for distances and angles is discussed in Proposition IV. Also given in Table V are the deviations of atoms in the anion from the best plane fitted to seven of the atoms.

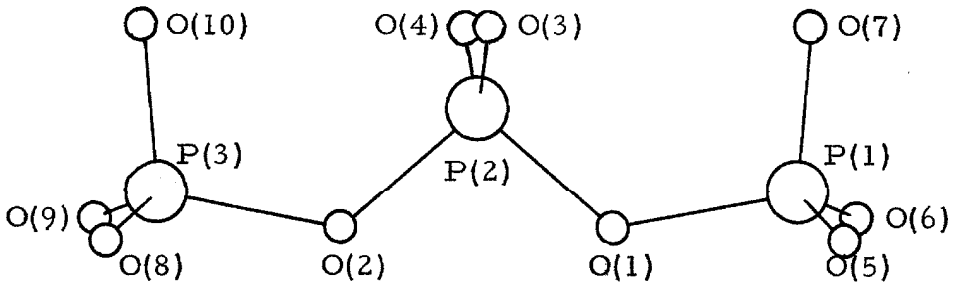

Figure 4. Triphosphate Ion.

Cruickshank[13] has calculated theoretical lengths for the bonds in the triphosphate ion. These are given in Table VI along with average observed lengths in various structures. The difference in length of the two types of bond in a middle PO_4 group is consistently much less than predicted although qualitatively in agreement with theory. The agreement with theory is excellent for the end PO_4 groups in $Na_5P_3O_{10} \cdot 6H_2O$. The present work confirms that in the triphosphate ion the lengths of the two types of chain bond differ much more than expected. The bond lengths in the three triphosphate structures agree fairly well, although in the Phase I structure their significance is limited by inaccuracy and a high degree of distortion.

Average values for certain types of bond angle in several phosphate structures are compared in Table VII. The angles in the Phase I structure are obviously anomalous.

In middle PO_4 groups, the bonds to the terminal oxygens are shorter, and the angle between them is larger than tetrahedral. The angle between the longer bonds to chain oxygens is less than tetrahedral. Other angles are nearly tetrahedral. In end groups, the bonds to terminal oxygens are also shorter and spread apart more. The observed increase in the bond angle as bonds get shorter and the negative charge on oxygen increases is to be expected because of electrostatic repulsion.

In the triphosphate ion end PO_4 group, among the three angles between the bond to the chain oxygen and the bonds to terminal oxygens, the one involving the terminal oxygen nearest to the terminal oxygens of the middle PO4 group is larger than the other two. The

increase in this angle is accompanied by a decrease in the opposite angle in the end group. These distortions are probably caused by electrostatic repulsion between the terminal oxygens of the middle group and the neighboring terminal oxygen of each end group.

Cruickshank[14] states that the POP angle of 122° in the anhydrous forms of sodium triphosphate is the smallest known for linked phosphate tetrahedra. The value of 123.5° in the hexahydrate is thus a little closer to that in other structures.

The triphosphate ion in the hexahydrate does not have twofold axial symmetry as it does in the anhydrous forms.

Table V. Distances and Angles in the Triphosphate Ion of $Na_5P_3O_{10} \cdot 6H_2O$

Interatomic Distances in Å:*

P(1)O(1)	1.649	P(3)O(8)	1.516
P(1)O(5)	1.521	P(3)O(9)	1.507
P(1)O(6)	1.516	P(3)O(10)	1.509
P(1)O(7)	1.509	P(1)P(2)	2.866
P(2)O(1)	1.596	P(2)P(3)	2.862
P(2)O(2)	1.589	O(3)O(7)	3.068
P(2)O(3)	1.502	O(3)O(10)	3.309
P(2)O(4)	1.491	O(4)O(7)	3.149
P(3)O(2)	1.667	O(4)O(10)	3.066

Angles in Degrees:*

O(1)P(1)O(5)	103.4	O(2)P(2)O(4)	111.3
O(1)P(1)O(6)	104.6	O(3)P(2)O(4)	118.1
O(1)P(1)O(7)	105.8	O(2)P(3)O(8)	102.4
O(5)P(1)O(6)	112.9	O(2)P(3)O(9)	105.1
O(5)P(1)O(7)	114.4	O(2)P(3)O(10)	105.7
O(6)P(1)O(7)	114.3	O(8)P(3)O(9)	114.0
O(1)P(2)O(2)	98.0	O(8)P(3)O(10)	114.0
O(1)P(2)O(3)	109.9	O(9)P(3)O(10)	114.0
O(1)P(2)O(4)	109.9	P(1)O(1)P(2)	124.1
O(2)P(2)O(3)	107.8	P(2)O(2)P(3)	122.9
		P(1)P(2)P(3)	151.44

* The standard deviations derived from the least squares refinement were less than .002 Å for interatomic distances and less than 0.1° for angles. The actual standard deviations should be somewhat larger due to systematic errors.

Table V (cont'd.)

Distance in Å from Each Atom to the Plane Fitted by Least Squares (with Equal Weights) to O(10), P(3), O(2), P(2), O(1), P(1), and O(7):

O(10)	.007	O(1)	.005	O(9)	-1.664
P(3)	-.219	P(1)	-.124	O(3)	1.387
O(2)	.225	O(7)	.008	O(4)	-1.174
P(2)	.096	O(8)	.729	O(5)	1.025
				O(6)	-1.484

Table VI. Theoretical and Average Observed PO Bond Lengths for Various Phosphates, in Å

	P(end) - O(terminal)	P(end) - O(chain)	P(middle) - O(terminal)	P(middle) - O(chain)
Theoretical Length[13]	1.51	1.65	1.45	1.64
$Na_5P_3O_{10}\cdot 6H_2O$	1.513±.008*	1.658±.010	1.496±.006	1.592±.004
$Na_5P_3O_{10}$, II[14]	1.50±.01	1.67	1.49	1.61
$Na_5P_3O_{10}$, I[3]	1.47±.03	1.66	1.52	1.62
$Na_4P_2O_7\cdot 10H_2O$ (15)	1.51±.02	1.61		
Six Long Chain Metaphosphates[16-21]			1.48±.06	1.60±.06

* The indicated range includes all individual values used in the average.

13 D. W. J. Cruickshank, J. Chem. Soc. 5486 (1961).

14 D. W. J. Cruickshank, Acta Cryst. 17, 674 (1964).

15 D. W. J. Cruickshank, Acta Cryst. 17, 672 (1964).

16 K. H. Jost, Acta Cryst. 16, 623 (1963).

17 K. H. Jost, Acta Cryst. 16, 640 (1963).

18 K. H. Jost, Acta Cryst. 14, 844 (1961).

19 K. H. Jost, Acta Cryst. 14, 779 (1961).

20 K. H. Jost, Acta Cryst. 15, 951 (1962).

21 D. W. J. Cruickshank, Acta Cryst. 17, 681 (1964).

Table VII. Average Observed Angles for Various Phosphates, in Degrees

End PO_4 Groups:

	O(chain)P - O(terminal)*	O(terminal)P - O(terminal)**
$Na_5P_3O_{10} \cdot 6H_2O$	103.9±1.5†, 105.8±.05	114.2±.24, 113.4±.6
$Na_5P_3O_{10}$, II[14]	101.3±1.2, 106.9	115.7±.7, 113.4
$Na_5P_3O_{10}$, I[3]	105.5±9, 118	109±10, 120
$Na_4P_2O_7 \cdot 10H_2O$[15]	105±2	113±2

Middle PO_4 Groups:

	O(terminal)P - O(terminal)	O(chain)P - O(chain)	O(chain)P - O(terminal)
$Na_5P_3O_{10} \cdot 6H_2O$	118.1	98.0	109.7±1.9
$Na_5P_3O_{10}$, II[14]	116.4	98.7	110.05±.05
$Na_5P_3O_{10}$, I[3]	115.8	93.8	111.3±1.6
Six Long Chain Metaphosphates[16-21]	118±4	100±3	109±8

P-O-P Angles:

$Na_5P_3O_{10} \cdot 6H_2O$	123.5±.6	$Na_4P_2O_7 \cdot 10H_2O$[15]	133.6
$Na_5P_3O_{10}$, II[14]	122.2	Six Long Chain Metaphosphates[16-21]	131±8
$Na_5P_3O_{10}$, I[3]	121.8		

* Where there are two values, the larger is for angles of the type O(2)P(3)O(10) in Figure 4, and the smaller is for the other two angles.

** Where there are two values, the smaller is for angles of the type O(8)P(3)O(9) in Figure 4, and the larger is for the other two angles.

† The indicated range includes all individual values used in the average.

Sodium Coordination

The sodium coordination polyhedra are illustrated in Figure 5. The associated distances and angles are given in Table VIII. There are two distorted octahedra, one distorted trigonal bipyramid, and two other distorted octahedra with only five of the corners occupied by ligands and the sixth corner replaced by a very long contact.

The International Tables[22] list observed ranges and average values for the sodium to oxygen distance. For the sixfold coordination in this structure, all Na-O distances are within the listed range, and the average value for each sodium ion is within .03 Å of the listed average. For fivefold coordination, the average value for each sodium ion is within .04 Å of the listed average and is, as expected, less than either value for sixfold coordination. Some individual values fall outside the listed range, but they are all greater than the lower limit listed for sixfold coordination and less than the upper limit listed for fourfold coordination. Thus, since the distances are expected to increase with increasing coordination number, the present values are still reasonable.

The average Na-O distance for each sixfold coordination polyhedron in sodium triphosphate hexahydrate also falls within the range observed in the anhydrous forms[2, 3]. No fivefold coordination was observed in the anhydrous forms.

Four of the ten oxygen atoms in the anion are not involved in

---

22 International Tables for X-Ray Crystallography, The Kynoch Press, Birmingham, England (1962), Vol. III, p. 258.

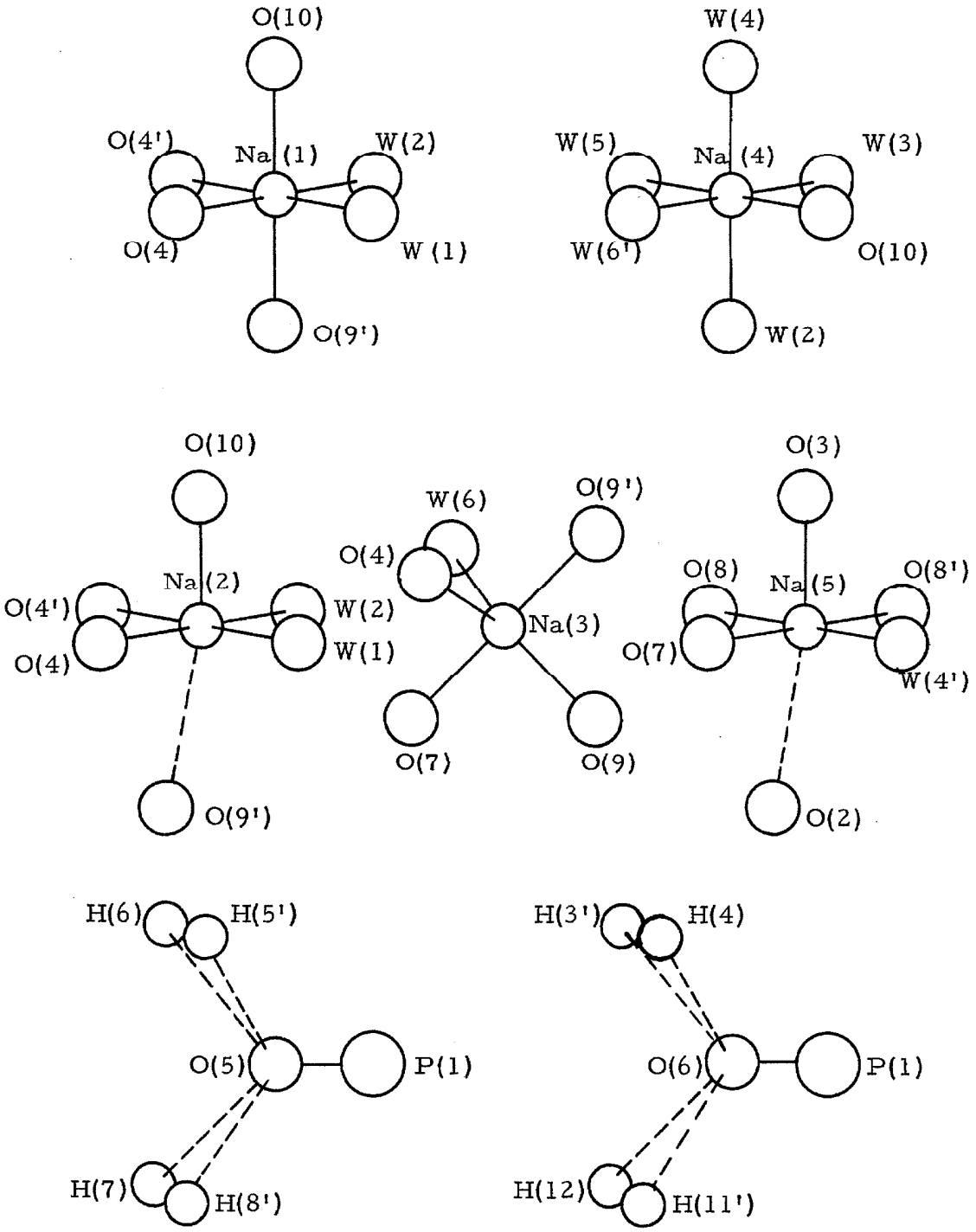

Figure 5. Sodium Ion Coordination and Configurations about O(5) and O(6).

Table VIII. Sodium Coordination Distances and Angles

Standard deviations derived from the least squares refinement are less than .004 Å and .15° for distances and angles involving W(5). For other distances and angles, they are less than .0025 Å and .1°. The actual standard deviations should be somewhat larger due to systematic errors.

Distances in Å:

Na(1)O(4')	2.467	Na(3)O(9)	2.325
Na(1)O(9')	2.489	Na(3)W(6)	2.449
Na(1)O(4)	2.373	mean	2.410
Na(1)O(10)	2.534		
Na(1)W(1)	2.457	Na(4)W(6')	2.439
Na(1)W(2)	2.360	Na(4)O(10)	2.373
mean	2.447	Na(4)W(2)	2.464
		Na(4)W(3)	2.435
Na(2)O(3')	2.393	Na(4)W(4)	2.450
Na(2)O(3)	2.367	Na(4)W(5)	2.322
Na(2)O(10)	2.344	mean	2.414
Na(2)W(1)	2.382		
Na(2)W(3)	2.301	Na(5)O(8')	2.435
mean	2.357	Na(5)W(4')	2.388
Na(2)O(2')	3.098	Na(5)O(3)	2.353
		Na(5)O(7)	2.483
Na(3)O(9')	2.392	Na(5)O(8)	2.307
Na(3)O(4)	2.401	mean	2.393
Na(3)O(7)	2.481	Na(5)O(2)	3.492

Angles in Degrees:

O(4)Na(1)O(10)	77.3	O(10)Na(2)W(1)	94.3
O(4)Na(1)W(1)	89.4	O(10)Na(2)W(3)	90.0
O(4)Na(1)O(4')	98.2	O(10)Na(2)O(3')	99.3
O(4)Na(1)O(9')	79.6	W(1)Na(2)W(3)	87.0
O(10)Na(1)W(1)	87.9	W(3)Na(2)O(3')	96.4
O(10)Na(1)W(2)	85.0	O(3)Na(2)W(3)	174.7
O(10)Na(1)O(4')	94.4	W(1)Na(2)O(3')	165.9
W(1)Na(1)W(2)	85.9		
W(1)Na(1)O(9')	94.7	O(4)Na(3)O(7)	80.3
W(2)Na(1)O(4')	87.1	O(4)Na(3)O(9)	135.6
W(2)Na(1)O(9')	118.3	O(4)Na(3)W(6)	107.9
O(4')Na(1)O(9')	86.1	O(4)Na(3)O(9')	81.0
O(4)Na(1)W(2)	161.8	O(7)Na(3)O(9)	106.3
O(10)Na(1)O(9')	156.7	O(7)Na(3)W(6)	81.0
W(1)Na(1)O(4')	172.4	O(9)Na(3)W(6)	116.5
		O(9)Na(3)O(9')	86.1
O(3)Na(2)O(10)	89.2	W(6)Na(3)O(9')	106.4
O(3)Na(2)W(1)	87.9	O(7)Na(3)O(9')	161.3
O(3)Na(2)O(3')	88.8		

Table VIII (cont'd.)

Angles in Degrees:

O(10)Na(4)W(2)	86.3	O(3)Na(5)O(7)	78.7
O(10)Na(4)W(3)	86.2	O(3)Na(5)O(8)	100.5
O(10)Na(4)W(4)	94.6	O(3)Na(5)O(8')	101.2
O(10)Na(4)W(6')	97.2	O(3)Na(5)W(4')	112.3
W(2)Na(4)W(3)	88.7	O(7)Na(5)O(8)	98.6
W(2)Na(4)W(5)	90.0	O(7)Na(5)W(4')	82.8
W(2)Na(4)W(6')	92.7	O(8)Na(5)O(8')	86.8
W(3)Na(4)W(4)	87.1	O(8')Na(5)W(4')	92.3
W(3)Na(4)W(5)	89.2	O(7)Na(5)O(8')	174.5
W(4)Na(4)W(5)	88.8	O(8)Na(5)W(4')	146.7
W(4)Na(4)W(6')	91.5		
W(5)Na(4)W(6')	87.5		
O(10)Na(4)W(5)	174.1		
W(2)Na(4)W(4)	175.6		
W(3)Na(4)W(6')	176.5		

sodium coordination, O(5) and O(6) because they are surrounded by hydrogen bonds, and O(1) and O(2) because they have very little negative charge. All other phosphate oxygens have two or three close sodium neighbors, and the water oxygens have from one to three.

Hydrogen Bonding

Only one hydrogen atom, H(1), does not form a hydrogen bond. The distances and angles describing the water molecules and the eleven hydrogen bonds are given in Table IX. The position of H(1) seems to be wrong, since both the distance W(1)H(1) and the angle H(1)W(1)H(2) are not very reasonable. Also, H(1) was slow to refine. Strangely, the temperature factor and standard deviations for H(1) seem normal. Because H(1) is unreliable and not involved in a hydrogen bond, it is excluded from the discussion which follows.

All HWH angles, except for W(1), are within a standard deviation of both the gas phase value[23] of 105.5° and the tetrahedral value. The average angle is very near the tetrahedral value. The average deviation of the WH distances from the mean is less than the estimated standard deviations, and the difference between the mean of 0.86 Å and the gas phase value[24] of 0.96 Å is due to the difference in position of the hydrogen nucleus and the centroid of its electron density.

---

[23] G. C. Pimental and A. L. McClellan, The Hydrogen Bond, W. H. Freeman and Co., San Francisco (1960), p. 264.

[24] Ibid., p. 259.

Table IX. Hydrogen Bond Distances and Angles*

Atoms	WO (Å)	WH (Å)	HWO (degrees)	OWO' (degrees)	HWH' (degrees)
W(1)H(1)**		.72±.05			88±7
W(1)H(2)O(8)	2.713±.003	.99±.05	9±3		
W(2)H(3)O(6')	2.969±.003	.81±.04	17.5±3	106.6±.1	110±6
W(2)H(4)O(6)	2.795±.003	.79±.04	10±4		
W(3)H(5)O(5')	2.891±.003	.84±.04	14±3	106.6±.1	111±6
W(3)H(6)O(5)	2.781±.003	.85±.04	8±3		
W(4)H(7)O(5)	2.812±.003	.81±.04	9±3	104.1±.1	109±6
W(4)H(8)O(5')	2.844±.003	.89±.06	4±4		
W(5)H(9)O(7)	2.797±.004	.86±.05	8±4	122.9±.2	107±7
W(5)H(10)O(1)	2.967±.004	.82±.05	12±4		
W(6)H(11)O(6')	2.872±.003	.93±.04	6±3	101.5±.1	107±6
W(6)H(12)O(6)	2.800±.003	.86±.05	3±4		
Mean†	2.840	.86	7	108	109

* Standard deviations are those derived from the least squares refinement. The actual standard deviations should be somewhat larger due to systematic errors.

** The nearest oxygen to W(1) besides O(8) is W(6'), which is 3.253 Å away.

† Excluding H(1).

Pimentel and McClellan[25] give an average WO distance of 2.75 ± 0.16 Å for hydrogen bonds formed by water in inorganic crystals. Only two of the hydrogen bonds deviate from this average by more than a standard deviation, and all deviations are less than 1.5σ. One of these two is a rather long bond accepted by O(1) which is expected to be a relatively poor acceptor because of its smaller negative charge. The average length is greater than 2.75 Å because O(5) and O(6) each accept four hydrogen bonds, resulting in more than the usual amount of repulsion among the hydrogen atoms. The lengths of the hydrogen bonds accepted by O(7) and O(8), each of which accepts one, are quite close to 2.75 Å.

The configurations about O(5) and O(6) are illustrated in Figure 5, and pertinent distances and angles are given in Table X. The shortest distance between hydrogen atoms in different water molecules is 2.49 Å, which is more than the van der Waals distance, 2.4 Å.[26] The angles POH vary between 104° and 127° with an average of 112.5°. It is rare for one covalently bonded atom to accept four hydrogen bonds, and the occurrence of two such atoms in this structure is the most interesting feature of the hydrogen bonding.

Although it is now generally accepted that the hydrogen bond is primarily electrostatic in nature, it has been proposed that its directional properties are determined largely by the directional properties of the lone pair orbitals of the acceptor atom, and that the strongest

(25) G. C. Pimentel and A. L. McClellan, The Hydrogen Bond, W. H. Freeman and Co., San Francisco (1960), p. 284.

(26) L. Pauling, The Nature of the Chemical Bond, Cornell University Press, Ithaca, New York (1960), 3rd Ed., p. 260.

Table X. Arrangement of Hydrogen Atoms about O(5) and O(6)

Distances in Å:*

O(5)H(6)	1.94 ± .04	O(6)H(3')	2.21 ± .05
O(5)H(5')	2.08 ± .04	O(6)H(4)	2.02 ± .05
O(5)H(8')	1.95 ± .05	O(6)H(11')	1.95 ± .04
O(5)H(7)	2.02 ± .04	O(6)H(12)	1.94 ± .05
H(6)H(5')	2.49 ± .06	H(3')H(4)	2.62 ± .06
H(5')H(8')	2.52 ± .07	H(4)H(11')	2.70 ± .06
H(8')H(7)	2.49 ± .07	H(11')H(12)	2.52 ± .07
H(7)H(6)	2.89 ± .06	H(12)H(3')	2.73 ± .07

Angles in Degrees:*

H(6)O(5)H(5')	76 ± 3	H(3')O(6)H(4)	76 ± 3
H(5')O(5)H(8')	77 ± 3	H(4)O(6)H(11')	86 ± 3
H(8')O(5)H(7)	77 ± 3	H(11')O(6)H(12)	81 ± 3
H(7)O(5)H(6)	93 ± 3	H(12)O(6)H(3')	82 ± 3
P(1)O(5)H(6)	120 ± 2	P(1)O(6)H(3')	108 ± 2
P(1)O(5)H(5')	105 ± 2	P(1)O(6)H(4)	127 ± 2
P(1)O(5)H(8')	105 ± 2	P(1)O(6)H(11')	112 ± 2
P(1)O(5)H(7)	119 ± 2	P(1)O(6)H(12)	104 ± 2
H(7)H(6)H(5')	89 ± 3	H(3')H(4)H(11')	94 ± 3
H(6)H(5')H(8')	91 ± 3	H(4)H(11')H(12)	86 ± 3
H(5')H(8')H(7)	98 ± 3	H(11')H(12)H(3')	96 ± 3
H(8')H(7)H(6)	83 ± 3	H(12)H(3')H(4)	83 ± 3

* The standard deviations, which were derived from the least squares refinement, should be increased somewhat to allow for systematic errors.

bonds result when the hydrogen bond direction is collinear with the lone pair orbital direction[27]. Obviously this is impossible for the hydrogen bonds to O(5) and O(6); and since these bonds are only slightly longer than usual, the importance of collinearity with the lone pair orbital direction is probably not as great as had been thought. Although similar orientations have been observed before[28-31], the implications of these previous structures for hydrogen bonding theory were not as great because the hydrogen bonds were much longer ($\geq$ 2.99 Å).

It is generally accepted[32] that the angle HWO, the deviation of the hydrogen bond from linearity, should not exceed ten or fifteen degrees. The three greatest deviations in $Na_5P_3O_{10} \cdot 6H_2O$ are for the three weakest hydrogen bonds; and the greatest, involving H(3), is still within a standard deviation of fifteen degrees. Otherwise, deviations are ten degrees or less.

The angle OWO', formed by a water oxygen atom and two oxygen atoms accepting hydrogen bonds from it, can vary widely. All such angles in this structure are reasonable. The only appreciable deviation from normal involves the long bond to O(1).

27 W. G. Schneider, J. Chem. Phys. 23, 26 (1955).

28 P. Vaughan and J. Donohue, Acta Cryst. 5, 530 (1952).

29 W. J. Siemons and D. H. Templeton, Acta Cryst. 7, 194 (1954).

30 I. Olovsson and D. H. Templeton, Acta Cryst. 12, 827 and 832 (1959).

31 R. Liminga and I. Olovsson, Acta Cryst. 17, 1523 (1964).

32 G. C. Pimentel and A. L. McClellan, The Hydrogen Bond, W. H. Freeman and Co., San Francisco (1960), p. 265.

Five water oxygens are surrounded, as expected, by two hydrogens and two sodium ions in distorted tetrahedral arrangements for for which the angles at the center vary from 89° to 134°. W(5) is surrounded by two hydrogens and only one sodium ion. The four atoms lie nearly in a plane and the angles at W(5) are 107° (HWH), 121°, and 129°. No water molecule accepts a hydrogen bond.

Packing

The previously described sodium coordination polyhedra share edges and corners to form an infinite sheet parallel to the (001) plane as shown in Figure 6. The indentations at Na(4) and Na(4') each accommodate an end of a triphosphate ion.

The parallel sodium sheets related by the unit cell vector $\vec{c}$ are interleaved by parallel sheets containing all of the water molecules. Five water molecules form the hydrogen bonding network shown in Figure 7, and the sixth, W(1), forms only one hydrogen bond to O(8).

The structure is built up of alternating sheets of sodium ions and of water molecules linked together by the triphosphate ions. The direction of the anion chain axis is approximately parallel to [101], and one vector between anions related by a center of symmetry is approximately $.05\,\vec{a} + .50\,\vec{b} + .36\,\vec{c}$. Although there were edges shared between sodium coordination polyhedra and phosphate tetrahedra in both anhydrous sodium triphosphate structures[2, 3], this does not occur in the hexahydrate.

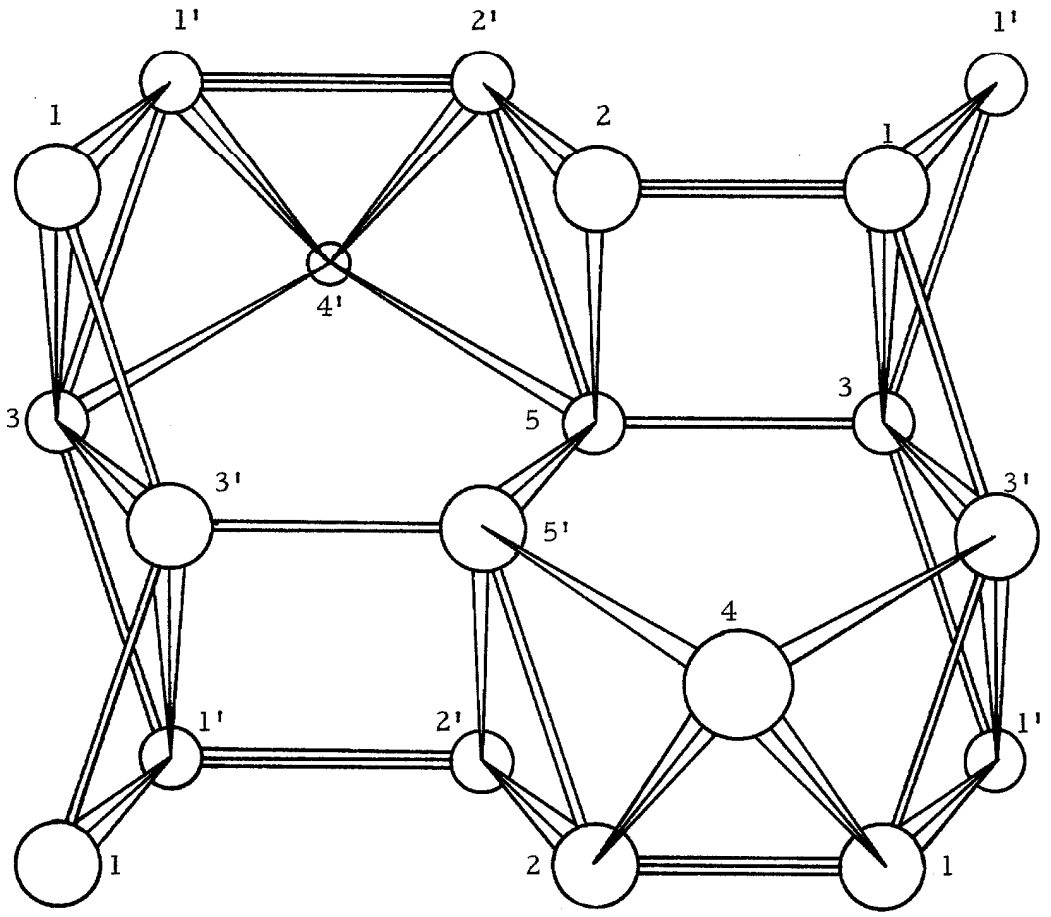

Figure 6. Sheet Structure of Sodium Coordination Polyhedra. Each polyhedron is represented by its sodium ion. Shared corners are designated by two lines connecting the sodiums, and shared edges are similarly designated by three lines.

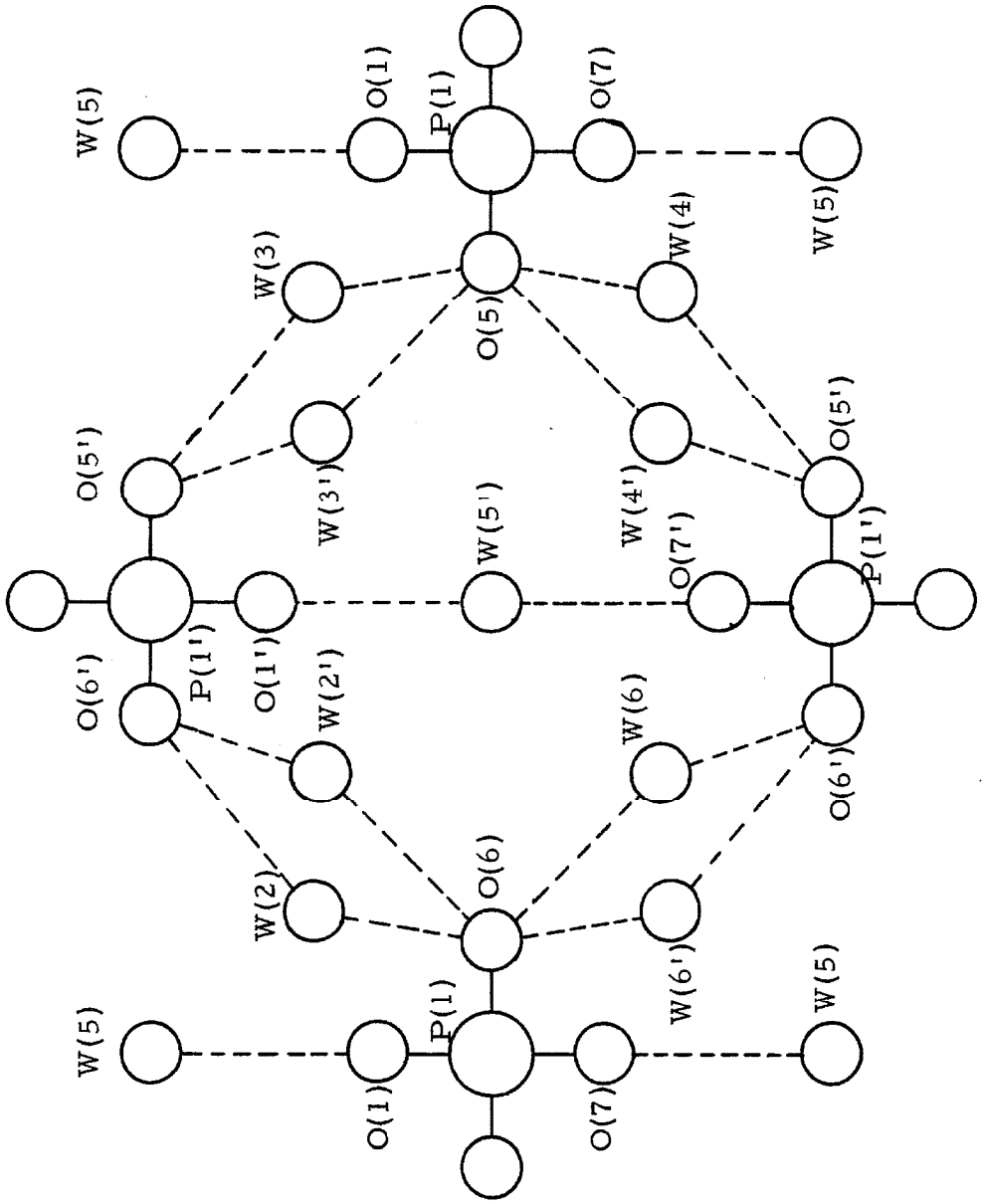

Figure 7. Hydrogen Bonding Network in c Projection. Covalent bonds are shown with solid lines; hydrogen bonds, with dashed lines.

Relation of Structure and Properties

Crystals of $Na_5P_3O_{10} \cdot 6H_2O$ are lath-like and limited by the three pinacoidal forms. The fastest growth is parallel to the b axis. This may be so because the orientation of the triphosphate ion in the unit cell is such that the area of contact between a growing pinacoidal face and an anion deposited from the solution, and hence the energy released upon deposition[33], is much greater for the (010) face than it is for the others. The slowest growth is parallel to the c axis. During growth of the (001) face in this crystal, a stage is reached in which the surface consists mainly of water molecules. At that point, the surface energy of the face must be relatively low because of the similarity between the solid surface and the solution. Thus, there is little impetus for further growth of the face. This could perhaps be changed by changing the nature of the solvent, thus changing the habit. The (001) face was also found to dissolve much more slowly than the other faces.

The best cleavage is parallel to the (010) face, probably because the phosphate chains are parallel to (010). There is a potential cleavage parallel to (001) which is resisted only by hydrogen bonds. Yet, this cleavage does not seem to be very good except at twin boundaries. There is a fair cleavage parallel to (100), probably because a plane parallel to (100) exists which does not cut a triphosphate ion.

Corbridge[3] postulated that the formation of twofold super-

---

33 L. V. Azároff, Introduction to Solids, McGraw-Hill Book Co., New York (1960), pp. 143-145.

saturated solutions by $Na_5P_3O_{10}$ II is due to an incomplete breakup of the structure yielding certain associated units in solution which are unfavorable for growth of the hexahydrate. The present work confirms that the associated units which were described would be unfavorable for growth of the hexahydrate, if they were to persist in solution.

The greater ease of hydration of Phase I is probably connected with the relative sodium ion coordination stabilities in the three sodium triphosphate structures, as was postulated by Corbridge[3]. Hydration of Phase II involves creation of fivefold coordination at the expense of sixfold coordination which is usually more stable; whereas hydration of Phase I involves the creation of fivefold and sixfold coordination in place of fourfold and sixfold coordination. No great similarities have been found between the Phase I and hexahydrate structures to help explain the greater hydration rate or the more rapid formation of hexahydrate crystals from solutions of Phase I. However, further comparison of the three structures may yet elucidate this and other phenomena such as the role of water in the formation of sodium triphosphate by calcination procedures[34].

Below 120° C, removal of the water from $Na_5P_3O_{10} \cdot 6H_2O$ results in hydrolysis of the triphosphate ion[35]. The rate of water loss is proportional to the surface area. The initial rate is very fast and temperature dependent; but after one or two moles of water are lost,

[34] J. R. Van Wazer, Phosphorus and Its Compounds, Interscience Publishers, New York (1958), Vol. I, p. 647.

[35] C. Y. Shen, J. S. Metcalf, and E. V. O'Grady, Ind. Eng. Chem. 51, 717 (1959).

the rate is slower, little affected by temperature, and apparently diffusion limited. Until more than a sixth of the water is lost, the crystals remain clear, and the hexahydrate is the only crystalline species present. There is an amorphous phase which contains considerable amounts of both anhydrous sodium triphosphate and degradation products. Hydrolysis apparently increases as more water is removed.

The extensive hydrolysis which always accompanies dehydration is probably due to a combination of anion instability and several features of the crystal structure. Anion instability may be due to weakness[2] of the bond P(end)O(chain) and to the flattened shape of the ends of the ion which facilitates backside attack upon the end phosphorus atoms. In the hexahydrate structure, W(5) has much more vibrational energy than any other part of the structure; and this water molecule is located directly adjacent to the end of the anion. Thus, as the structure breaks up, the most energetic water molecules are concentrated at positions suitable for attack upon the anions.

All the water is in layers parallel to (001) at one end of the anions. Suppose that as water is lost from these layers the rest of the structure tends to remain intact except for hydrolysis. This would prevent the growth of a crystalline anhydrous sodium triphosphate phase with its considerably different sodium coordination. Without the water, the remaining layers would get out of alignment and appear amorphous. The rate of water loss would be proportional to the surface area of the (100) and (010) faces and would be rapid and temperature dependent until the water near the surface was gone. Later, the water would have to diffuse greater distances between re-

maining layers, passing near the ends of many anions in the process and causing more hydrolysis. Hydrolysis products would probably tend to block the diffusion paths.

The crystal habit of hexahydrate crystals could greatly influence their properties. Normal crystals with their surface made up mostly of (001) faces should have relatively low rates of solution and dehydration with extensive hydrolysis during dehydration. However, if the relative amount of (001) surface were reduced by milling or by different conditions of growth, then for the same average particle size, the rates of solution and dehydration should be much higher while hydrolysis might be reduced.

The previously described twinning on the (001) face can be explained and clarified in terms of the crystal structure. The plane $z = 0.5$ does not cut a triphosphate ion and must lie near the twin boundary in this type of twin. Figure 8 shows a section of the structure from $z = 0.5$ to $z = 0.69$. Within the section there is a pseudo-twofold axis at Na(4') parallel to the c^* axis, although no such axis exists for the structure as a whole. Thus, if a single crystal were cut in two at the plane $z = 0.5$, one half could be rotated 180° about the axis through Na(4') and joined to the other half to form twins almost as stable as the single crystal. The twins are related by a 180° rotation about the c^* axis plus a translation of $2x_{Na(4')}\vec{a} + 2y_{Na(4')}\vec{b}$.

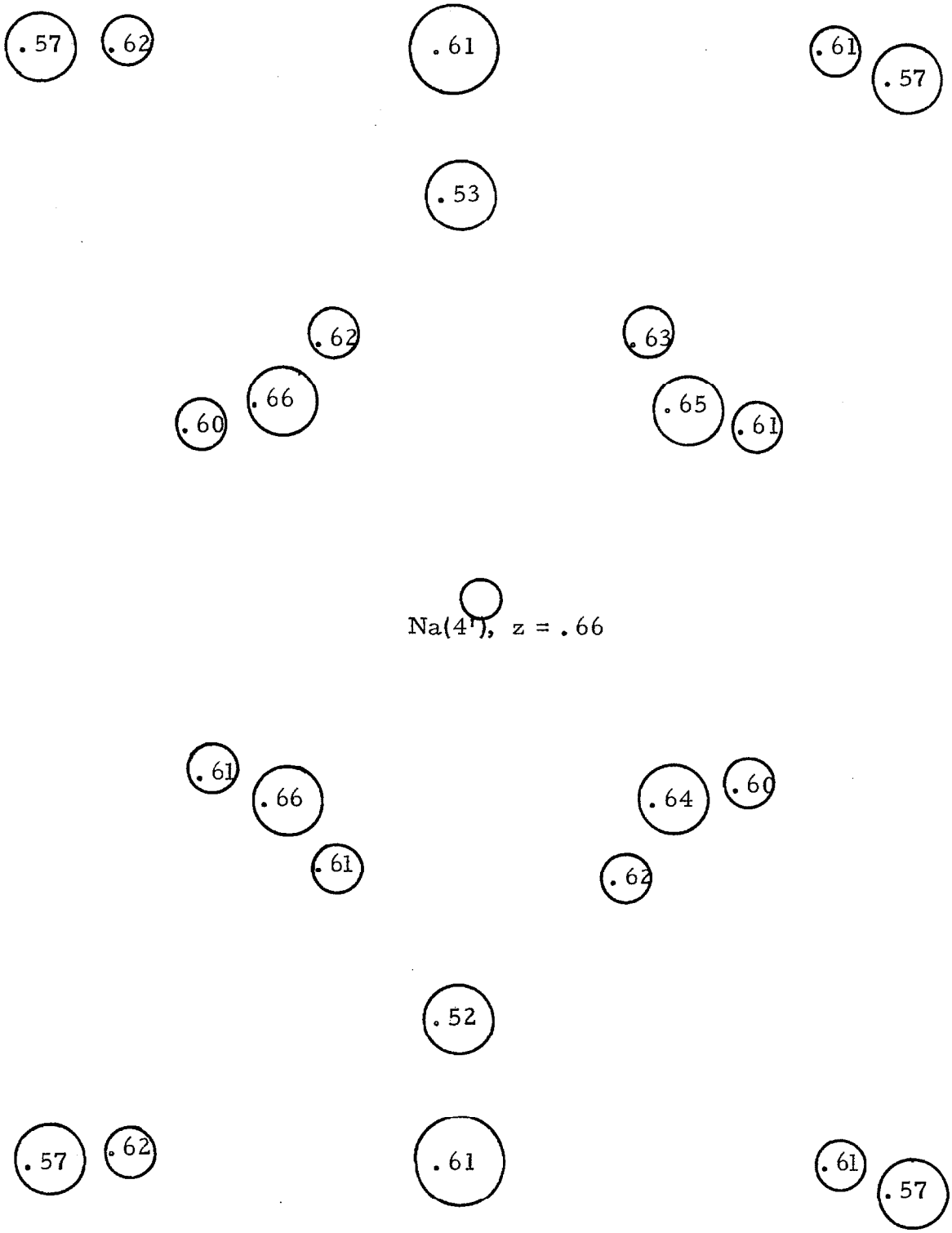

Figure 8. Section of Structure from z = 0.5 to z = 0.69. The value of z is given for each atom. Na, H, O, and P are shown as circles of increasing size.

PROPOSITIONS

PROPOSITION I

The Reynolds number for fluid flow is defined as $Re = DV\nu^{-1}$, where D is a characteristic length (diameter for a pipe or channel), V is an average velocity for the entire flow field, and ν is the kinematic viscosity of the fluid. Above a critical value of Re, the flow becomes turbulent with the degree of turbulence increasing with Re[36]. It is proposed to define a local Reynolds number Re' for each point in the flow field. No such concept could be found in the literature.

Define the local degree of turbulence T as the r.m.s. longitudinal velocity fluctuation, without dividing by the time-smoothed velocity as is customary[37]. Re' should be dimensionless, closely related to Re, calculable from the time-smoothed flow characteristics, and proportional to T.

The solid curves in Figure 9 show the observed variation of T over a cross section for flow between infinite parallel plates[38]. The most important feature is that T reaches a peak between the center and the wall. Similar behavior is assumed for pipe flow, although no data were found. Re' will first be discussed for pipe flow, for which an empirical velocity profile equation is available, and then applied to parallel plates for comparison with experiment.

For turbulent pipe flow in the range $10^4 < Re < 10^5$,

---

36 R. B. Bird, W. E. Stewart, and E. N. Lightfoot, Transport Phenomena, John Wiley and Sons, New York (1960), p. 41.

37 Ibid., p. 157.

38 J. Laufer, NACA Bull., Tech. Note 2123 (1950).

$$(1) \qquad \overline{V} = \overline{V}_{max}(1 - r/R)^{1/7}$$

where $\overline{V}$ is the time-smoothed longitudinal velocity and r/R is the distance from the center divided by the radius[39]. Using this equation, Re' was found to have a maximum at the center or at the wall if it was defined as $D\overline{V}\nu^{-1}$ or $D^2|\partial\overline{V}/\partial r|\nu^{-1}$ where D is the diameter or the distance to either the near or far wall. However, a satisfactory position of the maximum results if Re' is defined as

$$(2) \qquad Re' = D^n(D')^{(2-n)}|\partial\overline{V}/\partial r|\nu^{-1}$$

where $6/7 < n < 2$, D is the distance to the near wall, and D' is the distance to the far wall. Figure 10 shows the positional dependence of Re' for $n = 1$. If n is decreased, the maximum shifts toward the wall.

Using equation (1), it can be shown that

$$Re' = (\text{constant})(Re)(D/R)^{(n - 6/7)}(D'/R)^{(2 - n)} .$$

If Re' is averaged over a cross section of the pipe, the result is Re multiplied by a constant. Thus Re' is dimensionless and closely related to Re.

The reasons for the factors $|\partial\overline{V}/\partial r|$ and D^n in expression (2) are intuitively obvious, but the reason for the factor $(D')^{(2-n)}$ is not. One theory of turbulent flow says that energy is extracted from the mean flow mainly by the largest eddies and transferred from larger to smaller eddies where it is dissipated[40]. The greatest eddy

[39] R. B. Bird, W. E. Stewart, and E. N. Lightfoot, Transport Phenomena, John Wiley and Sons, New York (1960), p. 155.

[40] G. B. Schubauer and C. M. Tchen, Turbulent Flow, Princeton University Press, Princeton, New Jersey (1961), p. 6.

motion relative to the mainstream is at those parts of the outer edges of the eddy where eddy motion and mainstream motion are nearly parallel or antiparallel. Hence the rate of energy extraction and generation of turbulence at a point might be expected to increase with the size of the largest eddies which can exist with this point on the above mentioned parts of their outer edges. D' is equal to the diameter of such eddies if they are circular.

Re' and T calculated from experimental data[38] for flow between parallel plates at three values of Re are plotted versus r/R in Figure 9. Re' and T have been multiplied by different scale factors, but these scale factors and the exponent n are the same for all three values of Re . The positions of the maxima agree very well, and the peak heights for both Re' and T are proportional to Re . It is reasonable that the peaks in Re' are sharper than those in T since there is always some transfer of turbulence from high intensity regions to low.

To make the positions of the maxima agree exactly, the exponent n would have to be 1.21, 1.40, and 1.60 in order of increasing Re , instead of the single value of 1.4 used for Figure 9. This may indicate some dependence of n upon Re .

Re' rose to a second peak in the central region before dropping to zero at the center, probably because of errors in $|\partial\overline{V}/\partial r|$ which is very small there. It was reported[38] that the measured time-smoothed velocities were probably low where the turbulence was greatest. This would lead to erroneously high values of $|\partial\overline{V}/\partial r|$ in the central region. Using the excess of $|\partial\overline{V}/\partial r|$ over a small constant

instead of $|\partial\overline{V}/\partial r|$ would greatly lower Re' in the central region without affecting it much elsewhere.

Perhaps the laminar to turbulent transition occurs when Re' exceeds at any point some critical value which may or may not depend on geometry. Near the walls, a turbulent velocity profile has larger velocity gradients than does a laminar profile for the same bulk flow rate. If the maximum Re' were in this region for laminar flow with Re near its transitional value, a change to the turbulent velocity profile would result immediately in values of Re' greater than its critical value over an extended region. This would account for metastable laminar flow followed by a breaking into turbulence as Re is slowly increased.

Finally, Re' potentially provides a way to estimate T, and such things as turbulent heat or mass transfer coefficients which depend upon T, using only time-smoothed velocity data.

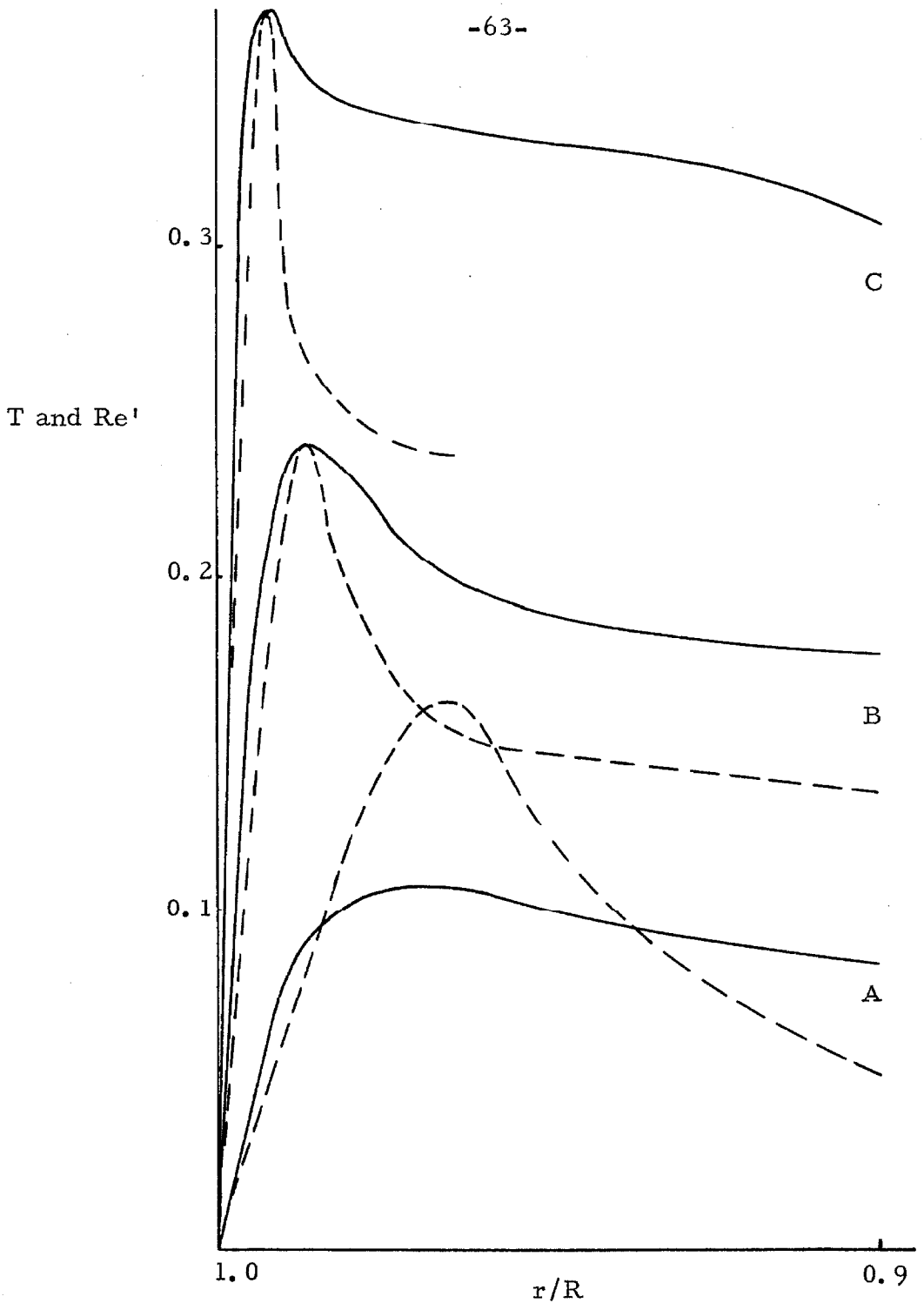

Figure 9. Observed Degree of Turbulence T (Solid Line) and Calculated Local Reynolds Number Re' (Dashed Line) Versus the Reduced Distance from the Center r/R . The flow is between parallel plates with Re equal to A. 12,300, B. 30,800, and C. 61,600. One arbitrary scale factor was applied to T ; another, to Re' .

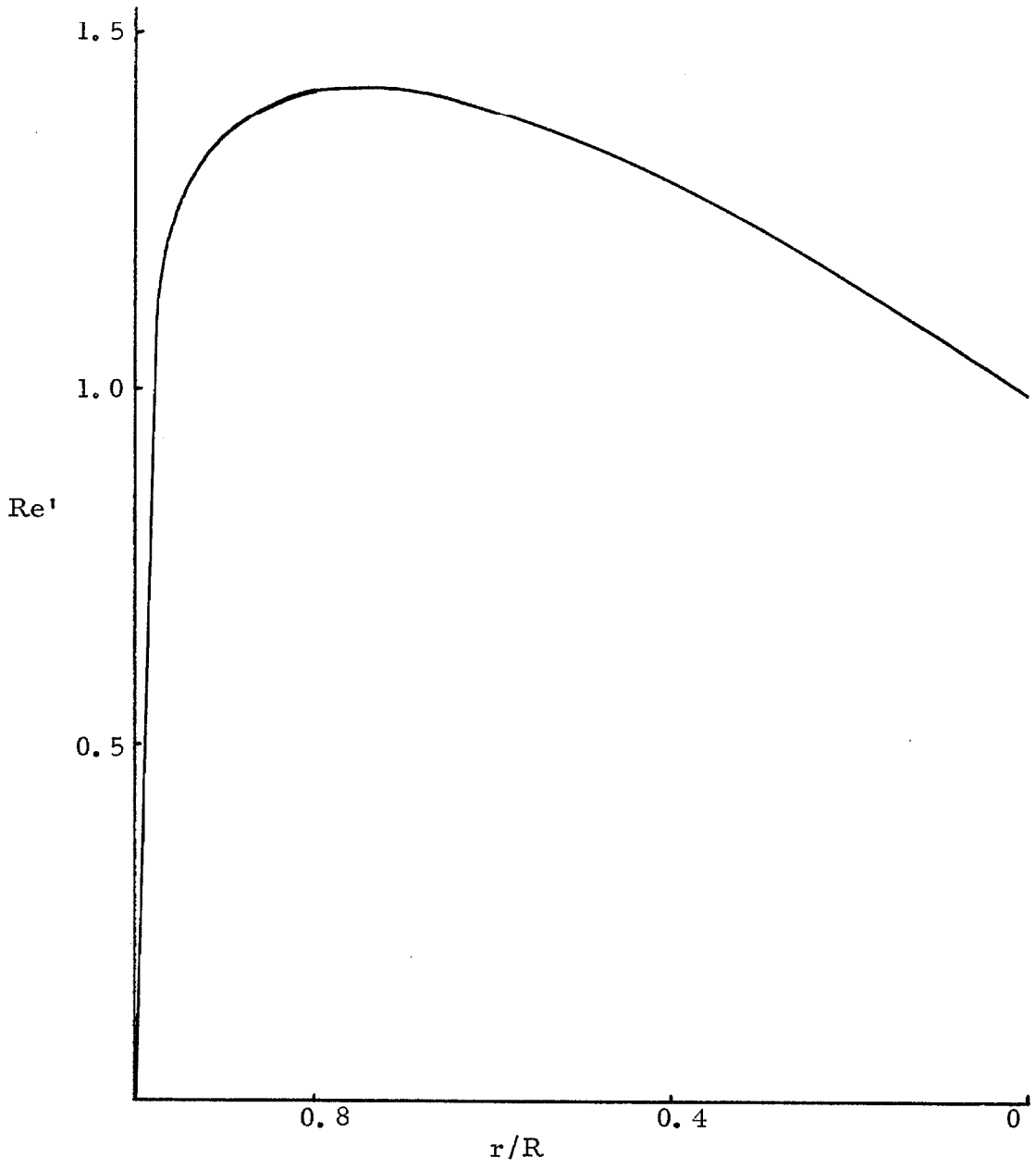

Figure 10. Local Reynolds Number Re' Versus the Reduced Distance from the Center r/R for Turbulent Pipe Flow with $10^4 < Re < 10^5$. Re' is on an arbitrary scale.

PROPOSITION II

Regular solution theory is discussed in detail in the recent monograph by Hildebrand and Scott[41]. A regular solution may have a nonzero heat of mixing, but the entropy of mixing at constant volume is ideal. Most nonpolar and weakly polar molecules form regular though nonideal solutions. A central problem is the calculation of $\Delta E_m = E_m - x_1 E_1 - x_2 E_2$ for binary solutions. At present, E_m is estimated by the equation

$$(3) \quad E_m = (x_1 V_1 + x_2 V_2)[(\Phi_1)^2 (\Delta E_v/V)_{11} + (\Phi_2)^2 (\Delta E_v/V)_{22} + 2\Phi_1 \Phi_2 (E/V)_{12}]$$

where E = cohesive potential energy per mole, ΔE_v = energy of vaporization, x = mole fraction, V = molar volume, m = mixing or mixture, and Φ = volume fraction. It is assumed that

$$(E/V)_{12} \simeq (\Delta E_v/V)_{11}^{\frac{1}{2}} (\Delta E_v/V)_{22}^{\frac{1}{2}} .$$

Equations of Langmuir[42-44] are said by Scatchard[45] to be equivalent except that empirical parameters replace the energies,

---

41 J. H. Hildebrand and R. L. Scott, Regular Solutions, Prentice-Hall, Englewood Cliffs, New Jersey (1962).

42 I. Langmuir, Chem. Rev. 6, 451-479 (1929).

43 I. Langmuir, Colloid Symposium Monograph III, 48-75 (1925).

44 J. A. V. Butler, D. W. Thomson, and W. H. Maclennan, J. Chem. Soc., 674-686 (1933).

45 G. Scatchard, Chem. Rev. 8, 321 (1931).

46 J. H. Hildebrand and R. L. Scott, Regular Solutions, Prentice-Hall, Englewood Cliffs, New Jersey (1962), p. 97.

with no reliable way of calculating the term for interaction of unlike molecules, and surface fractions replace volume fractions. Hildebrand and Scott[46] dismissed this surface fraction approach without offering a reason.

It is proposed to formulate regular solution theory in terms of surface fractions in order to take account of molecular size and shape and allow treatment of molecules with heterogeneous surfaces. A method of estimating molecular surface area is suggested, and theoretical and experimental justifications of the surface approach are offered.

Equation (3) was derived using assumptions which hold only for molecules of similar size and shape, and thus is not on a sound theoretical foundation for general application.

For nonpolar molecules, the pair potential is approximated by the London equation[47] and is proportional to the inverse sixth power of the separations of the interacting atoms. For normal aliphatic hydrocarbons in a liquid, about half the cohesive energy is due to hydrogen atoms alone. For molecules with larger surface atoms, the fractional contribution of the surface atoms is even greater; and in neopentane, the central atom's contribution is negligible.

Thus it is reasonable to think of the cohesive energy as distributed over a surface halfway between the two nearest molecular surfaces. In a mixture of molecules of types one and two, each having a homogeneous surface, this intermolecular surface is made up of

---

47 F. London, Trans. Faraday Soc. 33, 8 (1937).

three types (S_{11}, S_{22}, and S_{12}), each with a characteristic value of the energy per unit surface. With no space between molecules and random mixing, the fractional contributions to the total intermolecular surface are $S_{11}/\text{total } S = (\phi_1)^2$, $S_{22}/\text{total } S = (\phi_2)^2$, and $S_{12}/\text{total } S = 2\phi_1\phi_2$, where the surface fraction $\phi_i = x_i S_i/(x_i S_i + x_j S_j)$. Actual molecules with curved surfaces are associated with an intermolecular surface area larger than the molecular surface area. This tends to increase the fractional participation of the molecules with greater surface curvature, but it will be ignored as a first approximation. Thus,

(4) $E_m = (x_1 S_1 + x_2 S_2)[(\phi_1)^2(\Delta E_v/S)_{11} + (\phi_2)^2(\Delta E_v/S)_{22} + 2\phi_1\phi_2(E/S)_{12}]$,

assuming as before $(E/S)_{12} = (E/S)_{11}^{\frac{1}{2}}(E/S)_{22}^{\frac{1}{2}}$. This equation is of the same form as equation (3); and for molecules of equal surface to volume ratio, it will predict the same energy of mixing.

Molecular surface areas were estimated using known van der Waals radii, bond distances, and angles[48] as follows. Cyclopentane resembles a torus with $r = 2.00$ Å and $R = 3.365$ Å. The area assigned to a methylene group in a chain, 53.14 Å^2, is one fifth of the total area of such a torus. An end methyl is regarded as half a methylene plus a hemisphere of radius 2.00 Å. A side methylene or methyl adds an area equal to that of a chain methylene or end methyl minus a third of the area of the methylene to which it is attached. Areas of hydrocarbons are sums of the above quantities except that molecules such as methane and neopentane are regarded as spheres, and small rings are regarded as cylinders. The same methods are

---

48 L. Pauling, The Nature of the Chemical Bond, Cornell University Press, Ithaca, New York (1960), Ed. 3, pp. 260-261, 222-229, 311.

used for fluorocarbons with r increased by the factor $[\ell(C\text{-}F)+r(F)] \div [\ell(C\text{-}H)+r(H)]$. Surface areas are given in Table XI along with other quantities used in what follows.

In Figures 11 and 12, ΔE_v is plotted versus molar volume V and versus molecular surface area S respectively. All the molecules are very similar in makeup so that a straight line through the origin is expected when ΔE_v is plotted against a measure of the amount of effective attractive matter per mole. Figure 12 shows that S performs well as such a measure. However, in Figure 11, with V as the abscissa, the branched hydrocarbons fall off the curve; and although the normal hydrocarbons, because of the slowly varying surface to volume ratio, approach a straight line, the intercept at V = 0 is far below the origin.

In Table XII, the calculated compositions at which ΔE_m is a maximum for both volume and surface approaches are compared with experiment for various mixtures. The systems were chosen by Hildebrand and Scott[49] to illustrate the use of volume fractions; but whenever the predictions differ by more than 0.01, the surface fraction prediction is closer to the observed behavior.

In Table XIII are presented observed and calculated excess free energies for two binary mixtures involving appreciable differences in molecular shape. Hydrocarbons were chosen to assure validity of the geometric mean assumption for $(E/S)_{12}$. The surface fraction calculations and experimental values correspond to nearly ideal

---

[49] J. H. Hildebrand and R. L. Scott, Regular Solutions, Prentice-Hall, Englewood Cliffs, New Jersey (1962), p. 95.

solutions, but the volume fraction calculations predict appreciable positive values of F (excess).

Thus, both theory and experiment favor the surface fraction approach.

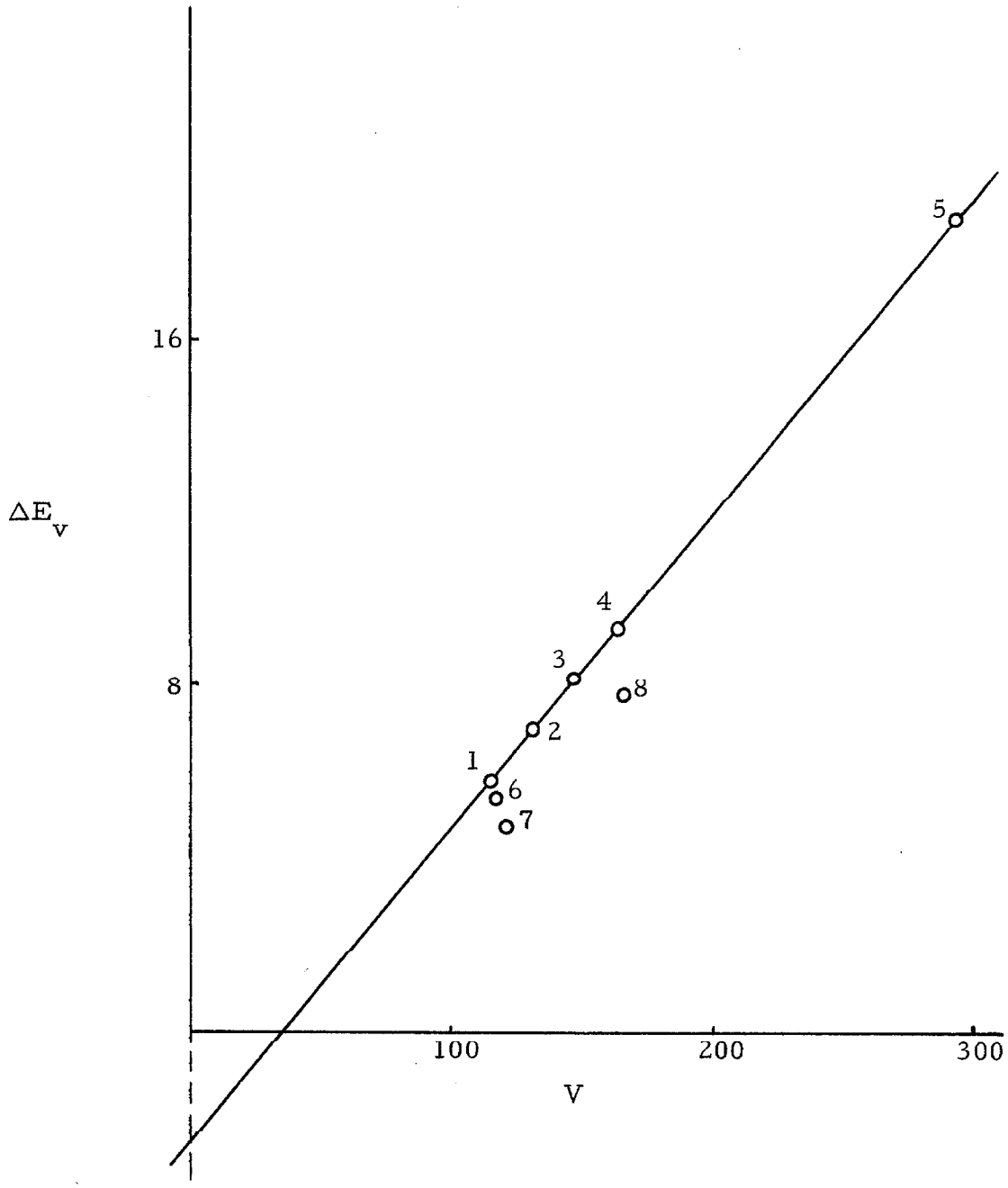

Figure 11. Energy of Vaporization ΔE_v (kcal/mole) Versus Molar Volume V (cm^3/mole). Individual points represent: 1. n-pentane, 2. n-hexane, 3. n-heptane, 4. n-octane, 5. n-hexadecane, 6. 2-methylbutane, 7. neopentane, 8. isooctane.

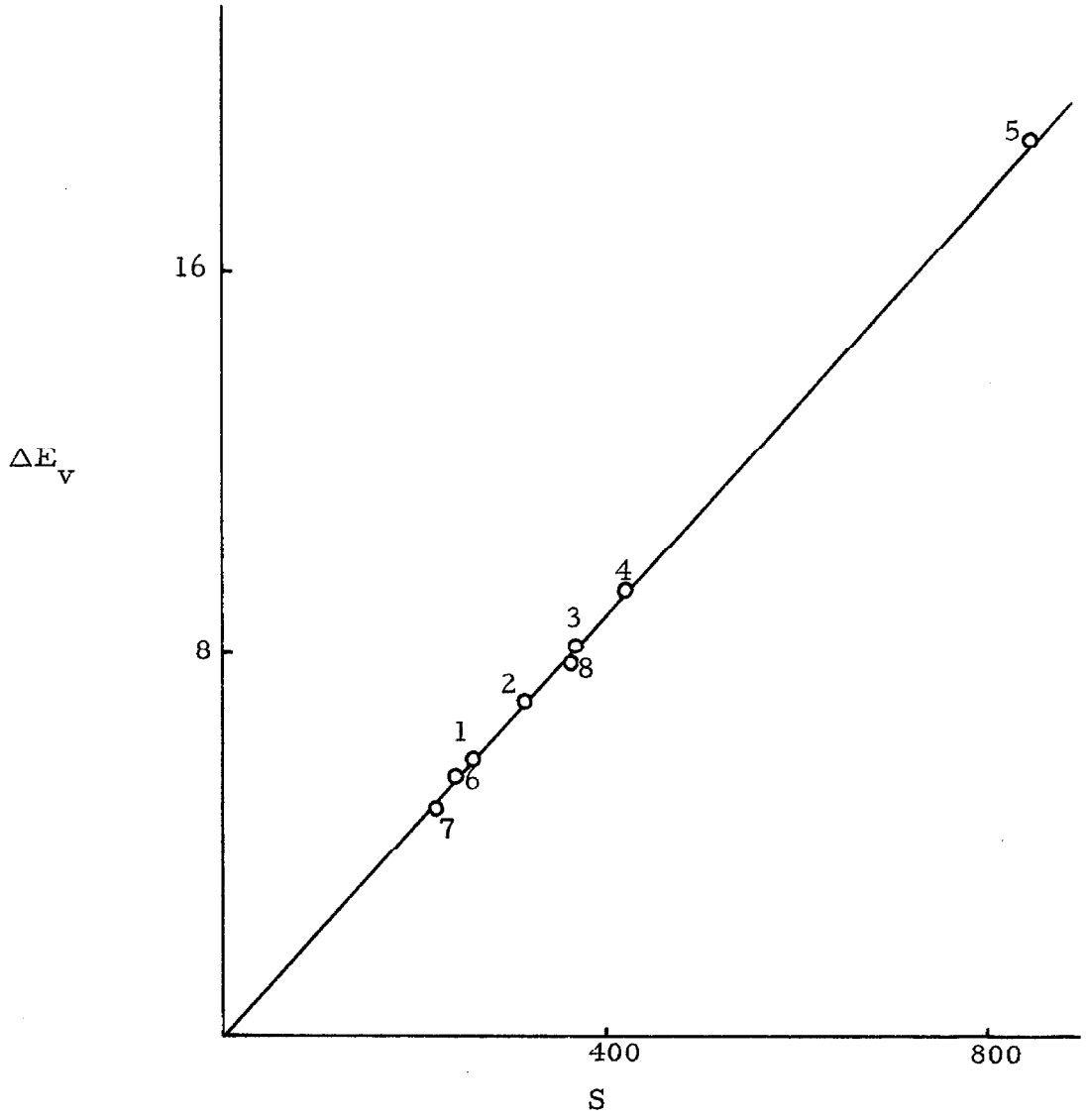

Figure 12. Energy of Vaporization ΔE_v (kcal/mole) Versus Molecular Surface Area S ($Å^2$/molecule). Individual points represent: 1. n-pentane, 2. n-hexane, 3. n-heptane, 4. n-octane, 5. n-hexadecane, 6. 2-methylbutane, 7. neopentane, 8. isooctane.

Table XI. Molecular Parameters

ΔH_v[50] and ΔE_v are the heat and energy of vaporization in kcal per mole. S is the molecular surface area in $Å^2$ per molecule. V is the molar volume in cm^3 per mole[50].

Substance	ΔH_v	ΔE_v	S	V	S/V	ΔE_v/S
n-C_6H_{14}	7.57	6.97	316	132	2.39	.02206
cyclohexane	7.91	7.31	192	109	1.76	.03812
n-$C_{16}H_{34}$	19.38	18.78	846	294	2.88	.02219
n-C_6F_{14}	7.75	7.15	418	205	2.04	.01710
n-C_7F_{16}	8.69	8.09	487	226	2.16	.01660
benzene	8.10	7.50	214	89	2.41	.03500
n-C_7H_{16}	8.75	8.15	369	147	2.51	.02208
isooctane	8.40	7.80	365	166	2.20	.02138
toluene	9.08	8.48	267	107	2.50	.03174
$CC\ell_4$	7.83	7.23	159.4	97	1.64	.04536
$SiC\ell_4$	7.19	6.59	182.5	115	1.59	.03611
n-C_5H_{12}	6.40	5.80	263	116	2.27	.02207
n-C_8H_{18}	9.92	9.32	422	164	2.58	.02207
2-methylbutane	6.03	5.43	244	117	2.08	.02228
neopentane	5.35	4.75	224.5	122	1.84	.02116

[50] J. H. Hildebrand and R. L. Scott, Regular Solutions, Prentice-Hall, Englewood Cliffs, New Jersey (1962), pp. 171-173.

Table XII. Composition Dependence of the Heat of Mixing ΔH_m

Experimental values of the mole fraction of component two for which ΔH_m is a maximum are compared to calculated values using surface (S) and volume (V) approaches(49). For the calculated values, it was assumed that the heat and energy of mixing would both be maximum at the same composition(51).

Component 1	Component 2	Observed	Calc. (V)	Calc. (S)
$n\text{-}C_6H_{14}$	cyclohexane	.60	.53	.56
$n\text{-}C_6F_{14}$	$n\text{-}C_6H_{14}$	.52	.55	.53$\overline{5}$
$n\text{-}C_7F_{16}$	isooctane	.51	.53	.54
benzene	$n\text{-}C_6H_{14}$	.45	.45	.45
benzene	cyclohexane	.50	.47	.51
benzene	$n\text{-}C_7H_{16}$	.45	.44	.43
toluene	$n\text{-}C_7H_{16}$	.50	.46	.46
$CC\ell_4$	cyclohexane	.47	.48	.48
$CC\ell_4$	$SiC\ell_4$	.60	.47	.48

51 J. H. Hildebrand and R. L. Scott, Regular Solutions, Prentice-Hall, Englewood Cliffs, New Jersey (1962), p. 102.

Table XIII. Comparison of Observed[52] Excess Free Energies F_E with Those Calculated by the Volume (V) and Surface (S) Approaches for Two Binary Mixtures

Component 1	n-heptane	n-octane
Component 2	isooctane	isooctane
Temperature (°C)	98.1	97.2
Mole Fraction of Component 1	.6195	.4811
Observed F_E (cal/mole)	-.367	-3.48
F_E Calc.* (S) (cal/mole)	+.498	+.565
F_E Calc.* (V) (cal/mole)	111.6	119.05
S/V , Component 1	2.51	2.58
S/V , Component 2	2.20	2.20

* $F_E \simeq$ energy of mixing at constant volume and temperature[51].

52 A. Beatty and G. Calingaert, Ind. Eng. Chem. 26, 504 (1934).

PROPOSITION III

For regular binary solutions, the excess free energy of mixing at constant temperature and pressure is approximately given[53] by

$$(5) \qquad F_E = \frac{x_1 S_1 x_2 S_2}{x_1 S_1 + x_2 S_2} \left[(E/S)_{11} + (E/S)_{22} - 2(E/S)_{12} \right] ,$$

where x = mole fraction, S = molecular surface area, and E = cohesive energy per mole. Cohesive energies for pure substances are approximated by the energy of vaporization[53]. The key problem is to calculate $(E/S)_{12}$ from the properties of the pure components.

The energy of interaction between two neutral atoms is given by the London equation[47]

$$(6) \qquad E_{12} = -3/2 \, \frac{\alpha_1 \alpha_2}{(r_{12})^2} \, \frac{I_1 I_2}{I_1 + I_2} ,$$

where α = polarizability, r_{12} = distance between centers, I = ionization energy. It is assumed[54] that r_{12} is the arithmetic mean of r_{11} and r_{22}.

In the most used treatment of regular solutions (which uses molar volume V instead of S), it is assumed that $(E/V)_{12}$ is the geometric mean of $(E/V)_{11}$ and $(E/V)_{22}$.[53] This requires assumptions that the sizes and ionization potentials are nearly equal, that molecules behave as neutral atoms, and that $V_{12} = (V_{11} V_{22})^{\frac{1}{2}}$. These bad assumptions lead to some spectacular failures.

---

53 J. H. Hildebrand and R. L. Scott, Regular Solutions, Prentice-Hall, Englewood Cliffs, New Jersey (1962), pp. 91, 102.

54 Ibid., p. 97.

Reed[55] attempts to allow for differing r and I, but incorrectly uses quantities which represent the molecules as wholes. The interaction between polyatomic molecules should instead be treated as a sum over atom pairs. This has been done for gases[56, 57] but not for liquids because straightforward integration over all orientations is not possible.

The new treatment proposed here eliminates all the bad assumptions above and uses an atom by atom approach. Other new considerations are a correction to the London equation by Pitzer[59], effects of molecular size and shape upon atom-atom interactions, and electrostatic interactions between molecules with no dipole moment. For simplicity, only tetrahedral (AB_4) or monatomic species are considered. Pertinent parameters are collected in Table XIV. The atom polarizabilities were estimated from experimental values[58] for various atoms and molecules, assuming additivity of atom polarizabilities in molecules.

Pitzer[59] has shown that for application of equation (6) to many electron atoms, one should use $I' = 1.15\ I$ for two electron systems and $I' = 2.25\ I$ for systems with SP closed shells. Also, "I" should be taken as an atomic rather than molecular parameter. In a

---

55 J. Reed, J. Phys. Chem. 59, 425 (1955).

56 S. Hamann, J. Lambert, and R. Thomas, Austr. J. Chem. 8, 149 (1955).

57 S. Hamann and J. Lambert, Austr. J. Chem. 7, 1 (1954).

58 Landolt-Börnstein, Zahlenwerte und Functionen, Springer Verlag, Berlin (1951), Vol. I, Part 3, p. 510.

59 H. Pitzer, Adv. Chem. Phys. II, 59 (1959).

homologous series, I (molecule) drops with increasing size, but the characteristic frequencies of the electrons, which I is meant to measure, probably don't change significantly.

Although the net dipole moments of the molecules considered here are zero, interaction of the partial charges on the atoms gives rise to significant potential energies. These are difficult to calculate because the ionic character of single bonds has been estimated only for bonds between univalent atoms and because the distance between molecules changes in an irregular manner with orientation since the molecules are in contact. There are also uncertainties due to possible double bond character.

A very rough estimate was obtained by calculating the energy for a single orientation assuming point charges of $n\delta$ on the outer atoms and $4n\delta$ on the central atoms. Here, δ is the charge calculated for a single bond between univalent atoms, and n is an arbitrary constant between one fourth and one. The total interaction energy is the sum over intermolecular atom pairs and over an average of 8.5 nearest neighbors[60] of the energies calculated by Coulomb's law and is given by an expression of the form

$$U(\text{cal/mole}) = 1.41 \cdot 10^{6} G n_1 n_2 \delta_1 \delta_2 \quad . \tag{7}$$

The calculated values of G are given in Table XIV. Values of U were between 39 and 300 cal/mole compared to values of F_E between 14 and 86 cal/mole.

In a pure liquid, the total London energy is assumed equal in

---

60 J. H. Hildebrand and R. L. Scott, Regular Solutions, Prentice-Hall, Englewood Cliffs, New Jersey (1962), p. 55.

magnitude to the energy of vaporization ΔE_v plus the Coulomb repulsion energy U. The London energy for a pair of molecules AB_4 and CD_4 is made up of four types: AC, AD, CB, and BD. It is assumed that AC is calculated exactly with equation (6) using Pitzer's I' and r (molecule) from Table XIV. BC is assumed equal to that calculated for a single atom B in contact with CD_4 divided by ϕ, where

$$(8) \qquad \phi(BC) = 2.356[r(CD_4)/r(AB_4)][\overline{AB}/r(B)]^{.5} - .971$$

for $.9 < \phi < 1.9$. AD is treated similarly. BD is assumed equal to the energy calculated for a pair of atoms B and D in contact divided by a constant. For a pure substance, this constant is chosen to give agreement of the total London energy with $\Delta E_v + U$. For unlike molecules, it is assumed to be the geometric mean of the constants for the two pure components. The London energy per pair of molecules is multiplied by 4.25 to obtain the energy in the liquid, assuming an average of 8.5 nearest neighbors[60].

The excess free energy is given by the equation

$$(9) \qquad F_E = \frac{x_1 S_1 x_2 S_2}{x_1 S_1 + x_2 S_2} [(E/S)_{11} + (E/S)_{22} - 2(E/S)_{12}]$$

$$- x_1 x_2 [U_{11} + U_{22} - 2U_{12}] .$$

It is assumed that $|U_{12}| = (U_{11} U_{22})^{.5}$ and $S_{12} = .5(S_{11} + S_{22})$.

The results of calculations for three mixtures are given in Table XV along with experimental values of F_E and values calculated by the old theory. Equation (8) may need revision as other mixtures are treated, but for these three it gives excellent agreement with experiment with reasonable choices of n. Methods of estimating ϕ and

U can probably be refined eventually to allow a priori predictions of F_E. Modifications will be necessary for other than tetrahedral molecules. The old theory is in complete disagreement with experiment for the systems in Table XV.

One very important qualitative conclusion which can be drawn from Table XV is that the interactions of the partial charges make contributions to F_E which are negative and large compared to F_E. Thus, it is possible to account for negative values of F_E. The old theory completely ignored such interactions and could predict only positive values of F_E, although negative values are often observed. The use of I' results in much weaker van der Waals interactions of hydrogen atoms with other atoms and leads to larger positive contributions to F_E for mixtures of hydrocarbons with molecules containing no hydrogen.

Table XIV. Physical Properties Used in Calculations

Van der Waals radii in Å [48, 61]: F = 1.35, CH_3 = 2.00, H = 1.2, Kr = 1.98

Bond lengths in Å [48]: CH = 1.095, CF = 1.385

Effective molecular radii* in Å: CH_4 = 2.00 Å, CF_4 = 2.385, Kr = 1.89

Surface areas = $4\pi r^2$ (effective) in $Å^2$: CH_4 = 50.3, CF_4 = 71.5, Kr = 44.95

Ionization potential in kcal/mole [62]: C = 259.5, H = 313.4, F = 401.5, Kr = 322.6

I' in kcal/mole [59]: C = 584, H = 360.3, F = 904, Kr = 726

Polarizabilities in $cm^3 \cdot 10^{25}$ [58]: C = 10.8, H = 3.95, F = 4.5, Kr = 25.08

Energy of vaporization in cal/mole [63-65]: CF_4 = 2890, Kr = 2006.7, CH_4 = 1992.8

Geometric factor G for equation (7): CH_4 = .048, CF_4 = .010

---

* For AB_4, $r_{eff.} = (\overline{AB} + r_B)\frac{2.00}{2.295}$. $r_{eff.}$ for Kr was estimated using ΔH_v and the London equation.

---

61 W. Keesom and H. Moody, Nature 125, 889 (1930).

62 L. Pauling, The Nature of the Chemical Bond, Cornell University Press, Ithaca, New York (1960), Ed. 3, p. 57.

63 R. Scott, J. Phys. Chem. 62, 136 (1958).

64 International Critical Tables, McGraw-Hill Book Co., New York (1926), Vol. I, p. 102.

65 International Critical Tables, McGraw-Hill Book Co., New York (1929), Vol. V, p. 136.

Table XV. Comparison of Observed[66] Excess Free Energies F_E with Those Calculated by the Present and Old[66] Theories

Component 1.	CH_4	CF_4	CH_4
Component 2.	Kr	Kr	CF_4
Observed F_E (cal/mole)	14	75	86
Present Calc. F_E (cal/mole)	14.5	75.4	85.0
Old Calc. F_E (cal/mole)	6	0	7
Contribution of the Change in London Energy to F_E (cal/mole)	+24.2	+134.0	+201.2
Contribution of the Change in Electrostatic Energy to F_E (cal/mole)	-9.7	-58.6	-116.2
n for Component 1	.6	.3	.6
n for Component 2	--	--	.3

66 N. Thorp and R. Scott, J. Phys. Chem. 60, 670 (1956).

PROPOSITION IV

Consider the estimation of standard deviations for the interatomic distances and bond angles in a structure based upon an orthogonal lattice. Assume that the standard deviations for the Cartesian coordinates of the atoms involved in each estimation are known and independent. Proposed here are a new corrected formula for the radial error of atomic position, a new formula for the standard deviation of a bond angle, and a new method of incorporating errors in the unit cell parameters into the analysis.

Here, ℓ_{ij} is the distance between atoms i and j ; θ_{ijk} is the angle at j formed by the lines from atom j to atoms i and k ; σ_i is the radial standard deviation of atom i ; and $\sigma(\Omega)$ is the standard deviation of Ω . The international Tables[67] give formulas for $\sigma(\ell)$ and $\sigma(\theta)$, taken from Cruickshank and Robertson[68], which require the calculation, for each atom, of positional standard deviations in many directions. This is very inconvenient, and commonly a single approximate radial standard deviation is used for each atom instead. Then the formula for $\sigma(\theta)$ can be simplified[69], and

$$(10) \qquad \sigma^2(\ell_{12}) = (\sigma_1)^2 + (\sigma_2)^2$$

$$(11) \qquad \sigma^2(\theta_{123}) = \frac{(\sigma_1)^2}{(\ell_{12})^2} + \frac{(\ell_{13})^2(\sigma_2)^2}{(\ell_{12})^2(\ell_{23})^2} + \frac{(\sigma_3)^2}{(\ell_{23})^2} \quad .$$

---

67 International Tables for X-Ray Crystallography, The Kynoch Press, Birmingham, England (1959), Vol. II, pp. 331-332.

68 D. W. J. Cruickshank and A. P. Robertson, Acta Cryst. 6, 698(1953).

69 S. F. Darlow, Acta Cryst. 13, 683 (1960).

Buerger[70] gives the following equation for σ_i when $\sigma(x_i) \simeq \sigma(y_i) \simeq \sigma(z_i)$

(12) $$\sigma_i = \sqrt{3}\,\sigma(x_i)$$

and seems to imply that it should be used for estimating standard deviations for bond distances and angles.

If the data used in the refinement of the structure are approximately spherically distributed about the origin in reciprocal space, the standard deviation of position for an atom along a particular arbitrary direction is expected to be approximately independent of direction provided that its vibrational ellipsoid is approximately spherical. Then $\sigma(x_i) \simeq \sigma(y_i) \simeq \sigma(z_i)$, and σ_i along any particular direction is given by

(14) $$\sigma_i = \sigma(x_i) \ .$$

It is this σ_i which should be used here rather than that given by equation (12).

Whittaker and Robinson[71] give the following expression for σ of the product of A and B where A has mean a and standard deviation σ_1, B has mean b and standard deviation σ_2, and ρ is the coefficient of correlation.

(13) $$\sigma^2(AB) = b^2(\sigma_1)^2+a^2(\sigma_2)^2+2\rho ab\sigma_1\sigma_2+(\sigma_1)^2(\sigma_2)^2(1+\rho)$$

---

70 M. J. Buerger, Crystal Structure Analysis, John Wiley and Sons, New York (1960), pp. 622, 634.

71 E. J. Whittaker and G. Robinson, The Calculus of Observations, Blackie and Son, London (1940), Ed. 3, p. 328.

Let ℓ' be the length of a bond in an assumed unit cell with cell parameters equal to those measured experimentally, and let d' be the repeat distance for the assumed cell in the direction of the bond. Let ℓ and d be the corresponding quantities in the actual cell. Then $\ell = \ell'(d/d')$, and using expression (13),

$$\sigma^2(\ell) = (\ell')^2\sigma^2(d/d') + (d/d')^2\sigma^2(\ell') + \sigma^2(d/d')\sigma^2(\ell') \ .$$

But $d/d' \simeq 1$, and because d' is not variable, $\sigma^2(d/d') = [\sigma(d)/d']^2$. Also, if K is the largest fractional error in a cell edge, $\sigma(d)/d' \lesssim K$. Thus,

$$\sigma^2(\ell) \simeq K^2(\ell')^2 + (1+K^2)\sigma^2(\ell') \simeq K^2(\ell')^2 + \sigma^2(\ell') \ ,$$

and using equation (10),

$$\sigma^2(\ell_{12}) = (\sigma_1)^2 + (\sigma_2)^2 + K^2(\ell'_{12})^2 \ . \tag{15}$$

To estimate the maximum error in θ_{123} due to an error of one standard deviation in the relative placement of atoms one and two, consider atom two fixed at the center of a circle of radius ℓ_{12} with all of the error occurring in atom one in a direction tangent to the circle. Assuming isotropic errors, the tangential displacement equals $\sigma(\ell_{12})$; and for reasonably small errors, the error in θ in radians equals $\sigma(\ell_{12})/\ell_{12}$. A similar result applies to atoms two and three, and certainly

$$\sigma(\theta_{123}) < \sigma(\ell_{12})/\ell_{12} + \sigma(\ell_{23})/\ell_{23} \ . \tag{16}$$

Expression (16) is much easier to use than expression (11) and will usually exceed it by less than a factor of two to give an estimated $\sigma(\theta)$ small enough for all practical purposes. In some cases involving small θ or a relatively large σ_2, expression (11) should be used if $\sigma(\theta)$ seems too large.

Equations (14) through (16), supplemented occasionally by equation (11), form a conveniently integrated treatment of the errors in the distances and angles of a structure. Of course, for symmetry related atoms, equation (15) must be appropriately modified.

PROPOSITION V

An empirical method is proposed for correlating the dipole moments of a series of molecules CH_nX_{4-n}, where the atoms X are halogen atoms. Estimates of the molecular quadrupole moments of the nonpolar molecules were obtained for use in regular solution theory. Unfortunately, these were wrong for reasons which will be discussed, but some modification of the same general approach may yet succeed in giving these quadrupole moments.

The plot of μ/er_o versus electronegativity difference Δy in Figure 13 was prepared using microwave spectroscopy data[72, 73] on the dipole moment μ and internuclear distance r_o for nine diatomic molecules composed of hydrogen and halogen atoms. Some electronegativities were adjusted by one or two tenths to give a smoother curve. The values used are: H = 2.0 , I = 2.5 , Br = 2.8 , Cℓ = 3.1 , and F = 3.8 .

Then, using microwave spectroscopy data[74-81] on the dipole moments and structures of nine different molecules CH_nX_{4-n}, the

---

[72] C. H. Townes and A. L. Schawlow, Microwave Spectroscopy, McGraw-Hill Book Co., New York (1955), pp. 13-14.

[73] L. Pauling, The Nature of the Chemical Bond, Cornell University Press, Ithaca, New York (1960), Ed. 3, pp. 78, 99.

[74] S. L. Miller, L. C. Aamodt, G. Dousmanis, C. H. Townes, and J. Kraitchman, J. Chem. Phys. 20, 1112 (1952).

[75] R. J. Myers and W. D. Gwinn, J. Chem. Phys. 20, 1420 (1952).

[76] S. N. Ghosh, R. Trambarulo, and W. Gordy, J. Chem. Phys. 20, 605 (1952).

[77] D. R. Lide, Jr., Phys. Rev. 87, 227 (1952).

[78] O. R. Gilliam, H. D. Edwards, and W. Gordy, Phys. Rev. 75, 1014 (1949).

[79] Q. Williams, J. T. Cox, and W. Gordy, J. Chem. Phys. 20, 1524 (1952).

effective electronegativity of carbon in each molecule was calculated and found to be linearly related (Figure 14) to an empirical function $(\log \sum_{i=1}^{4} 15^{y_i})$ of the electronegativities of the four attached atoms.

For predictions of molecular dipole or quadrupole moments, Figure 14 gives the effective electronegativity of carbon which can be used with Figure 13 to estimate the ionic character of the bonds. The good fit in Figure 14 indicates that dipole moments can then be successfully predicted. However, the fractional ionic characters predicted for the bonds in the nonpolar molecules are: $CH_4 = .12$, $CI_4 = .109$, $CBr_4 = .103$, $CC\ell_4 = .099$, and $CF_4 = .082$. This unreasonable result indicates that although molecular dipole moments can be predicted, the individual bond moments are wrong.

This is certainly connected with the oversimplified point charge model used for the molecular dipole moments. The factor which probably causes the most trouble is the atomic moment of the carbon atom which is opposed to the molecular moment and increases with ionic character, thus tending to equalize the molecular moments[82]. This factor must be partly responsible for the variation in the effective electronegativity of carbon, and because it operates similarly in all the dipolar molecules, its effects are apparently adequately treated in them. However, this contribution vanishes in nonpolar molecules leading to anomalous results.

[80] A. L. McClellan, Tables of Experimental Dipole Moments, W. H. Freeman and Co., San Francisco (1963), p. 37.

[81] C. H. Townes and A. L. Schawlow, Microwave Spectroscopy, McGraw-Hill Book Co., New York (1955), pp. 613-623.

[82] W. Gordy, W. V. Smith, and R. F. Trambarulo, Microwave Spectroscopy, John Wiley and Sons, New York (1953), p. 293.

It would be very useful to refine this treatment to allow estimation of the quadrupole moments of nonpolar molecules. These can potentially be estimated using collision cross sections determined by crossed molecular beam techniques or by pressure broadening of microwave spectra[83, 84]. However, only a very small number of simple molecules have been studied, none of which are of the type considered here, and the values obtained are not very accurate. Nuclear quadrupole coupling constants and nuclear magnetic resonance chemical shifts are also related to the ionic character of bonds, but the relationships are not yet well enough understood[85, 86]. The chemical shifts in CH_3CH_2Z are related to the electronegativity of the entire substituent group Z[87]. If this method could be developed to give reliable electronegativities for $-CX_3$ and $-X$, then the molecular quadrupole moment in CX_4 should be proportional to the difference.

In the present treatment, the molecular dipole moments should probably be increased by an amount proportional to the dipole moment before calculating the effective electronegativity of carbon for use in the nonpolar molecules. How this can be done remains to be worked out, and at least a few experimental quadrupole moments

---

83 W. V. Smith, J. Chem. Phys. 25, 510 (1956).

84 H. Feeny, W. Madigosky, and B. Winters, J. Chem. Phys. 27, 898 (1957).

85 J. D. Roberts, Nuclear Magnetic Resonance, McGraw-Hill Book Co., New York (1959), p. 26.

86 L. Pauling, The Nature of the Chemical Bond, Cornell University Press, Ithaca, New York (1960), Ed. 3, p. 100.

87 B. P. Dailey and J. N. Shoolery, J. Am. Chem. Soc. 77, 3977 (1955).

may be required. Meanwhile, the method can be applied as it stands to the dipole moments for series of tetrahedral molecules based upon carbon or its congeners.

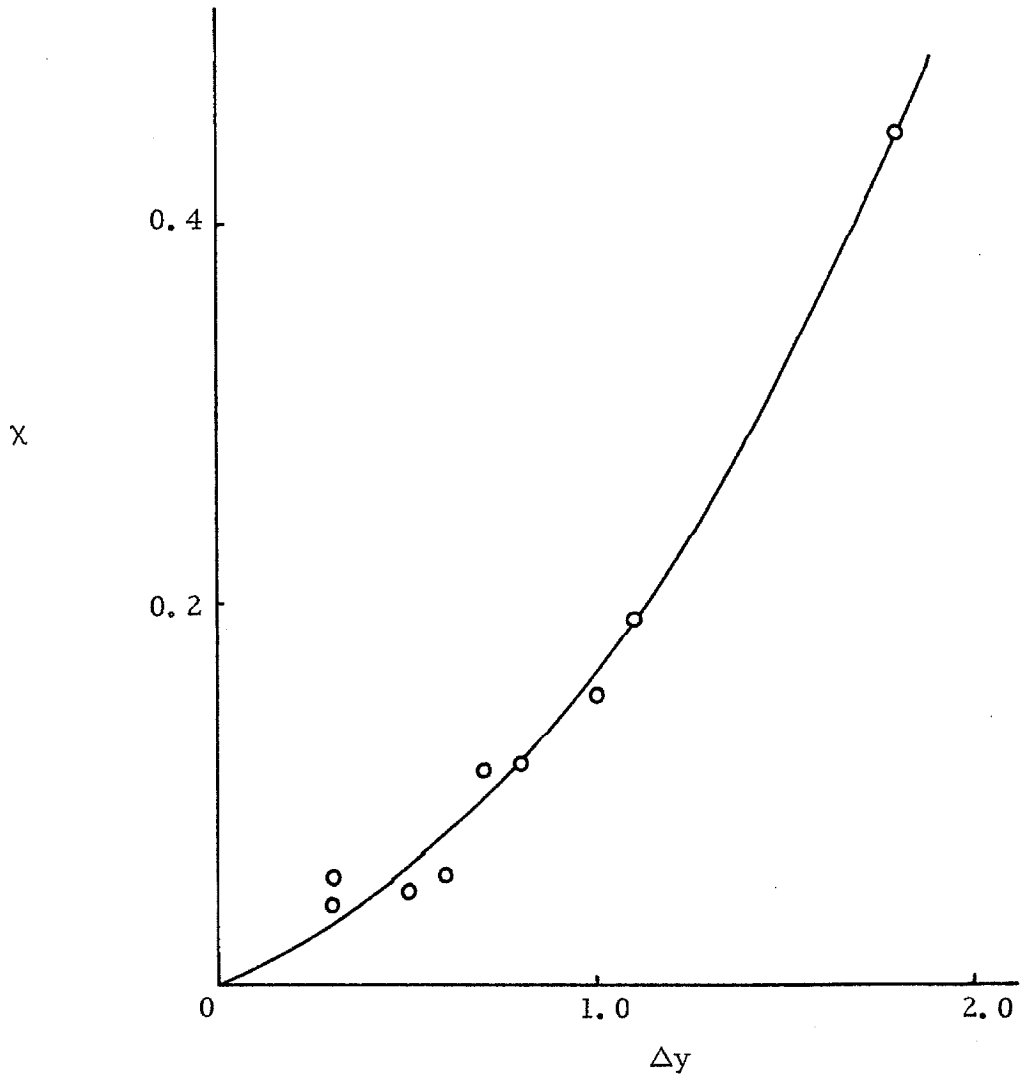

Figure 13. Ionic Character χ Versus Electronegativity Difference Δy for Certain Diatomic Molecules. Points in order of increasing ionic character represent the molecules BrI, HI, BrCℓ, ICℓ, CℓF, HBr, BrF, HCℓ, and HF.

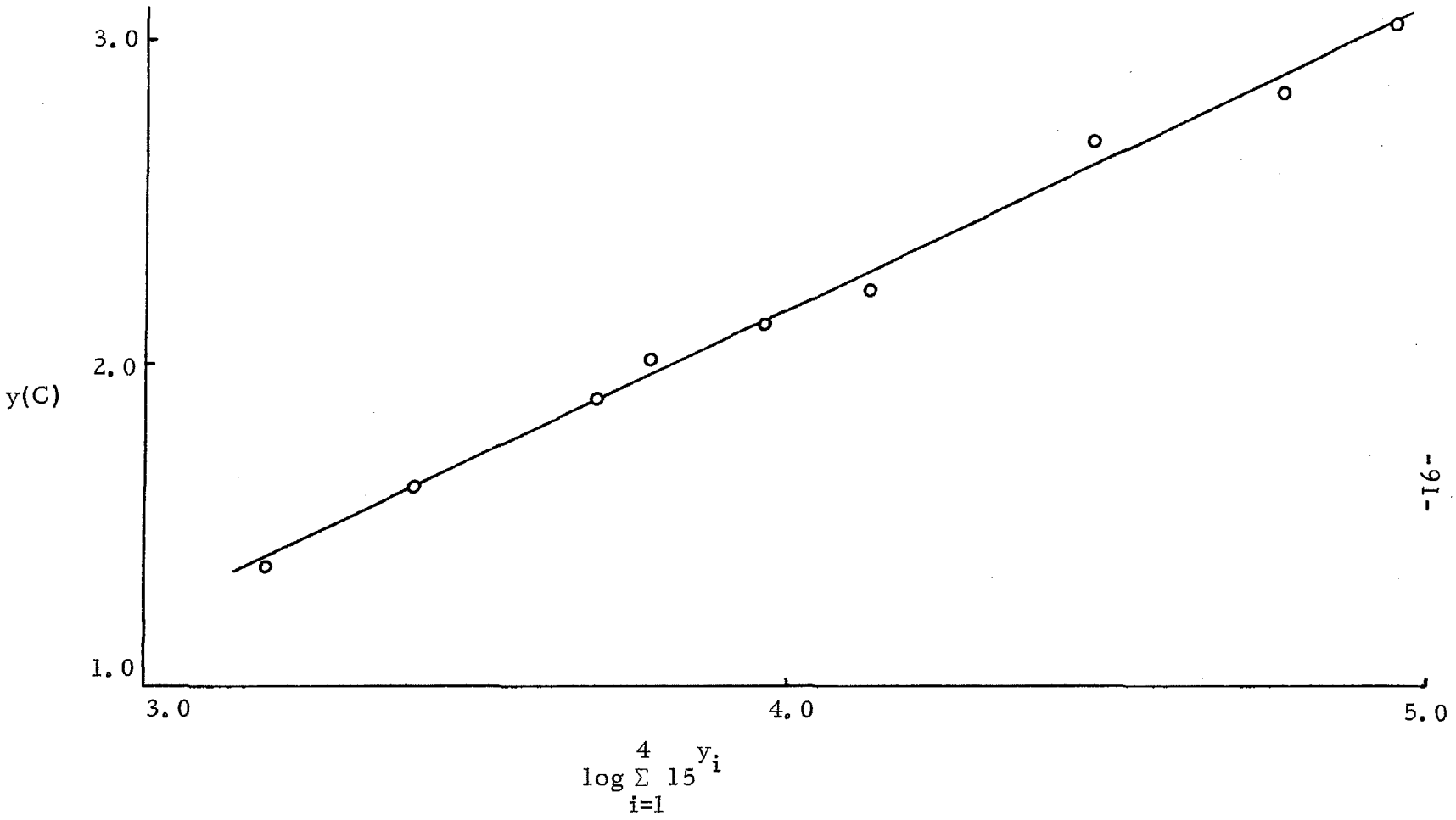

Figure 14. Effective Electronegativity of Carbon y(C) in Molecules CH_nX_{4-n} Versus the Function ($\log_{\sum_{i=1}^{4}} 15^{y_i}$) of the Electronegativities of the Four Attached Atoms. Points in order of increasing y_c represent the molecules CH_3I, CH_3Br, CH_3Cl, $CHBr_3$, CH_2Cl_2, $CHCl_3$, CH_3F, CH_2F_2, and CHF_3.

APPENDIX A

On pages A-2 through A-5 are listed the reflections which were observed as equal to some value and those which were observed as less than some value but were calculated to be larger than that value. On pages A-6 through A-9 are listed the reflections which were both observed and calculated to be less than some value. The only reflections which were considered which are not in this list are the low angle data given in Table II on page 6.

The data are in groups with common values of the indices h and ℓ, which are given in a heading at the beginning of each group. The numbers describing each reflection are, from the left, the value of k, the observed value of F times ten, and the final calculated value of F times ten. A minus sign for F_{obs} indicates that F was observed to be less than one tenth of the listed value. An asterisk indicates that the reflection has zero weight.

A-2

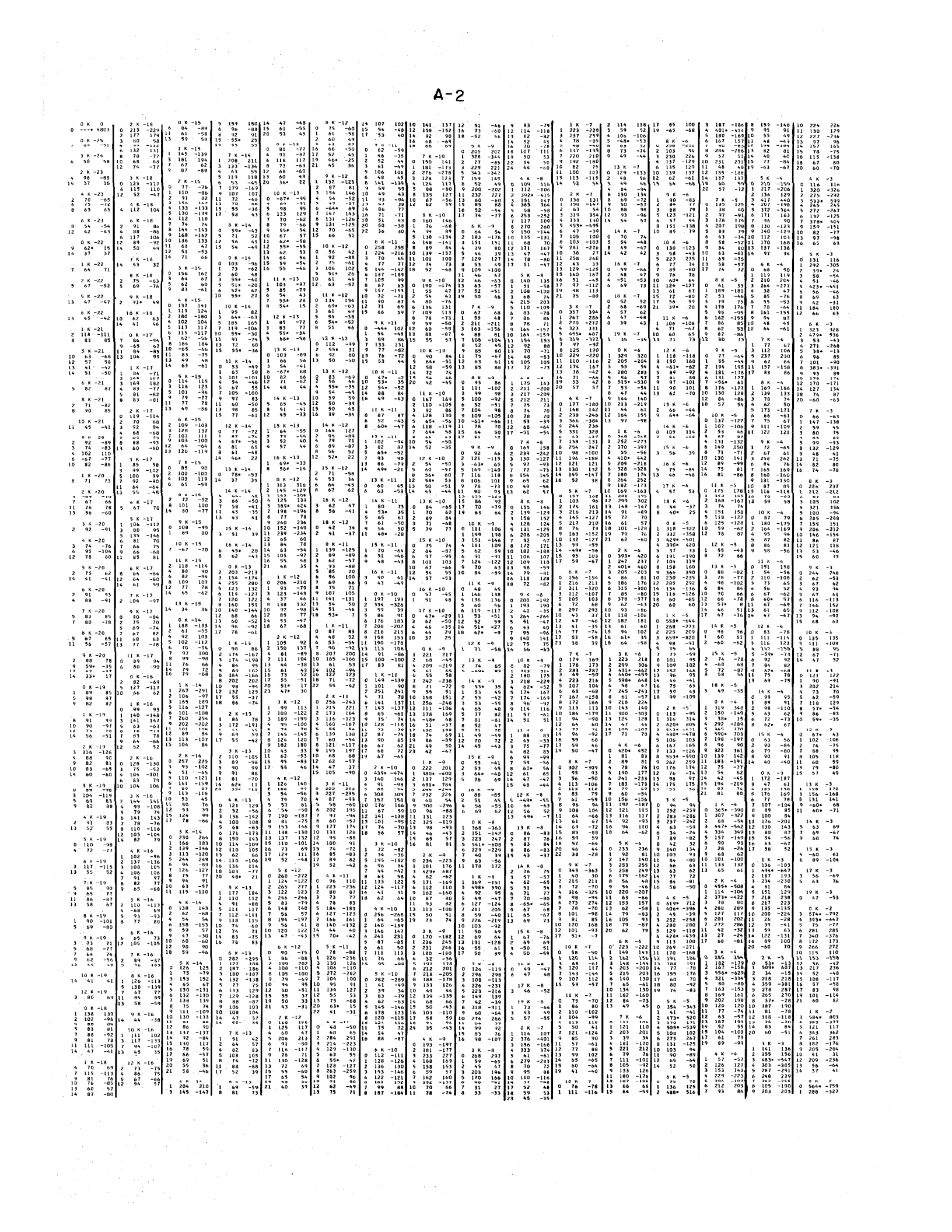

A-3

A-4